AFOSR-TR- 79-0456

(5) LEVEL II

Final Technical Report
1 March 1973 - 30 September 1978

ARPA Order No.: 3291
Program Code: 7F10
Contractor: Saint Louis University
Effective Date of Contract: 1 March 1973
Contract Expiration Date: 30 September 1978
Amount of Contract: $254,459
Contract Number: F44620-73-C-0042
Principal Investigators: Brian J. Mitchell
Otto W. Nuttli
Phone: 314-658-3123 or 3124
Program Manager: Brian J. Mitchell
Short Title: Research in Seismology

Sponsored by

Advanced Research Projects Agency (DOD)

ARPA Order No. 3291

Monitored by AFOSR Under Contract #F44620-73-C-0042

The views and conclusions contained in this document are those of the authors and should not be interpreted as necessarily representing the official policies, either expressed or implied, of the Defense Advanced Research Projects Agency or the U.S. Government.

Table of Contents

Research Objectives

Several lines of research have been pursued which pertain to (1) the properties of sources within continental interior regions and near the borders of plates, and (2) the nature of seismic wave propagation in various types of tectonic provinces. The former topic has involved research on M_S vs m_b relationships, scaling laws, and source mechanism characteristics for earthquakes. The latter topic has required the development of new methods for determining seismic wave attenuation coefficients, and has resulted in new Q models for various tectonic regions. Details of source properties and propagation effects have involved comparisons of theoretical spectra and seismograms for various sources with the corresponding observed quantities. Details of this work are presented in the following paragraphs.

Summary of Research Accomplished During the Contract Period

I. Introduction

During the period of this contract (April 1, 1973 to September 30, 1978) research has been conducted which relates to magnitude determination, spectral characteristics of seismic phases, and to the effects which various source characteristics, earth properties, and structural parameters have upon those phases. Research has been pursued using both body waves and surface waves, in various tectonic regions. Much effort has been devoted to the study of regional differences in source properties and propagation effects among earthquakes and explosions which occur in shield-like regions such as the central United States and stable portions of Eurasia, and tectonically active regions, such as southern Asia and active subduction zones.

II. Spectral studies

Central United States earthquakes.

This work has dealt with spectral and amplitude studies of earthquakes within the central United States between 1961 and mid-1974. Events ranging from m_b = 0.5 to m_b = 4.9 are relatively scaled by the vertical component of their Lg waves and empirically related to one of the seismic source parameters, and the seismic moment. Many of the larger of the earthquakes so scaled were also investigated for their focal mechanism solutions.

Spectra of more than three hundred short-period, vertical-component Lg waves of 78 earthquakes in the central United States were determined. From these, an empirical relationship between the long-period level of the Lg displacement spectrum and seismic moment were developed. There is a consistency between the corner period and the seismic moment, which implies a uniformity of earthquake processes in the central United States over a wide range of event sizes as opposed to California where wide variations in the corner period

are observed for source spectra having the same seismic moment. Due to the development of the corner period versus seismic moment behavior, the body- and surface-wave magnitude scales can be related.

The focal mechanism solutions for earthquakes in central United States suggest that local stress fields are important in determining the type and orientation of faulting. The implied stress system is considerably more complicated than that which would be produced by east-west trending compressive stresses, or northeast-southwest rifting, as previously suggested.

Eurasian Explosions and Earthquakes.

Two questions were posed in this study: 1) What is the physical reason that the m_b:M_S criterion is able to distinguish between earthquakes and explosions, 2) What is the physical explanation for earthquakes that are anomalous by the m_b:M_S criterion? In answer to the first, we found that in the frequency domain earthquakes and explosions of the same M_S are virtually indistinguishable. It is only in the time domain that the amplitude of the single pulse, explosion-generated P wave is larger than that of the more prolonged P wave of the typical earthquake of the same M_S value. In search of an answer to the second question, four anomalous Eurasian earthquakes were studied. For three the spectra were similar to those of typical earthquakes of the same M_S value. The only difference showed up in the time domain, where the P waves of the anomalous earthquakes consisted of a single pulse, similar to explosions, instead of a train of waves. For the same M_S, the amplitude of the single pulse P wave was greater than that of the more typical train of P waves. One anomalous earthquake, however, had a P-wave spectrum that was richer in the high frequencies (smaller corner period) than that of a typical earthquake of the same M_S. Thus it appears that earthquakes can be anomalous by the m_b:M_S criterion either because of a single pulse P-wave motion or because of an enrichment of the high frequency part of the spectrum.

To arrive at these conclusions, the spectra of P and Rayleigh waves of earthquakes and explosions were studied to determine how the spectra are affected by source properties, how the 1-sec and 20-sec spectral amplitude levels scale with m_b and M_S, and how the spectra of earthquakes which are anomalous by the m_b:M_S criterion compare to those which are not anomalous.

Spectra of P waves recorded at teleseismic distances for NTS events in tuff and rhyolite indicate an apparent T/Q of 1.0. For Piledriver, an NTS event in granite, and for USSR explosions in Kazakh, the apparent T/Q for P waves is approximately 0.8. Although the method of analysis employed to determine apparent T/Q values may not yield exact values, it is adequate to establish that T/Q for Piledriver and for Kazakh events is less than for NTS events in tuff and rhyolite. At 1-sec period the difference in spectral amplitude corresponding to the difference in T/Q values is 0.3 logarithmic units, or about a factor of two. This suggests that yield estimates of Kazakh and NTS granite explosions will be two times too large if based on an empirical curve of yield versus m_b for NTS events in tuff and rhyolite. The difference in apparent T/Q values may result from an actual difference in absorption in the source region, or it may be a consequence of more efficient coupling for NTS granite and Kazakh explosions.

Because absorption does not have much effect on spectral amplitudes at 20-sec period, yield estimates based on M_S or on the 20-sec P-wave spectral amplitudes should not show much dependence on the absorptive properties of the source region. One possible exception is a high-yield explosion such as Boxcar. We found its 20-sec P-wave spectral amplitude to be normal, but its M_S value to be anomalously large. The greater-than-normal excitation of surface waves may result from such causes as release of accumulated tectonic stress or relatively large spall and slap down. Yield estimates based on M_S thus could be anomalously large for such high-yield events.

Both for Eurasian earthquakes and for NTS and Kazakh explosions it usually was found that 1-sec P-wave spectral amplitudes scale as m_b (a tenfold increase in spectral amplitude causes a unit increase in m_b), and that 20-sec P-wave spectral amplitudes scale as M_S. As noted previously, the P-wave spectra of explosions and earthquakes of the same M_S are nearly identical; but the time-domain amplitudes of 1-sec period P-wave motion are larger for explosions than earthquakes.

None of the earthquakes and explosions considered had an M_S greater than 6.7. The M_S values, determined from time-domain measurements of Rayleigh waves, scaled directly as the seismic moments, which were determined from the P-wave spectra. (An exception was Boxcar.) From the work of other investigations we would expect that this scaling would break down when M_S exceeds 8, at which value the M_S scale becomes saturated.

Some earthquakes have anomalous m_b:M_S values, i.e., their M_S is relatively small compared to their m_b value. When m_b is plotted versus M_S, these earthquakes fall in or near the explosion population. P-wave spectra of such anomalous, as well as typical or normal, Eurasian earthquakes were studied to determine if the anomalous condition in the time domain also shows up in the frequency domain. For three earthquakes which had anomalous m_b:M_S values, the P-wave spectra were not anomalous, i.e., the spectra had the same shape as a typical or normal earthquake of the same M_S. Examination of the seismograms of these three earthquakes indicated that the P waves were characterized by a short time duration, compared to non-anomalous earthquakes. This single pulse (as contrasted to a train of waves) apparently results in a relatively large time-domain amplitude compared to a spectral amplitude at 1-sec period, which gives rise to an anomalously large m_b but not to an anomalously large spectral amplitude. This single-pulse

P wave probably is associated with earthquakes having relatively brief rupture times and small fault dimensions.

One Eurasian earthquake was found which was anomalous by the m_b:M_s criterion and which had an anomalously large 1-sec P-wave spectral amplitude. This earthquake apparently had a spectrum rich in high frequency motion (small corner period), as would be associated with high stress drop earthquakes.

Thus we can say that earthquakes which have anomalous m_b:M_s values may or more not have anomalous P-wave spectra, depending on whether the earthquakes are of short duration or of high stress drop.

III. Surface wave attenuation

Fundamental-mode studies at intermediate periods.

North America. The attenuation data for this region are more numerous than they are for any other region of the world. The attenuation coefficients for eastern and central North America were obtained from data for eight events. Surface waves from those events were recorded by between 24 and 42 seismograph stations in the United States and Canada. Mean attenuation coefficient values and the associated standard deviations for Rayleigh which traverse eastern and central North America vary between about 0.6×10^{-4} km^{-1} at 5-second periods to less than 0.1×10^{-4} km^{-1} at 40-second periods. Love wave attenuation coefficients over this period range are similar to the Rayleigh wave values. Standard deviations for these values typically range between 0.1 and 0.2×10^{-4}. Studies of attenuation in the western United States have indicated that significant regional differences in attenuation occur at periods less than about 16 s and that the differences become more pronounced with decreasing period.

The eastern United States attenuation coefficient determinations are of sufficient quality for inverting to obtain a model of Q_β^{-1}. In addition, the attenuation coefficient differences between eastern and western North America

were inverted to obtain a model for ΔQ_β^{-1}, the difference in internal friction as a function of depth between eastern and western North America. That difference was then used to infer a Q_β^{-1} model for western North America. The two models were found to differ by about a factor of 2 in the upper crust, western North America being more highly attenuating than eastern North America. The lower crust exhibits very low values for both regions. It is difficult to distinguish between the different Q_β^{-1} values, which are both very low, but it is possible that Q_β^{-1} in the lower crust may not be greatly different for the two regions.

Eurasia. Surface waves generated by eight Asian events (six earthquakes and two nuclear explosions, one atmospheric and one underground, as recorded by Eurasian stations) have been used to study the anelastic attenuation coefficients of the fundamental Rayleigh and Love wave modes. The paths from the sources to the stations are mainly continental and cross shield and tectonic regions.

Rayleigh wave amplitude data yielded average attenuation coefficients at periods between 4 and 50 seconds. The attenuation data show large standard deviations and in some cases the average attenuation coefficients show negative values due to regional variations of the attenuative properties of the crust, multipathing and scattering. Love wave amplitude data from two earthquakes, for which the focal mechanisms were evaluated, exhibit poor correlation between the observed and theoretical radiation patterns.

A method was developed to investigate the regional variation in the attenuative properties of the Eurasian crust and its effect on surface wave amplitude data, employing the evaluated average attenuation coefficients for the fundamental Rayleigh mode. For that investigation, Eurasia was divided into two regions; the first region, of shield type, incorporates all shield areas in Eurasia, and the second region, of tectonic type, incorporates the mountainous

areas and the fold systems of Eurasia. This regionalization shows that the shield-like regions are similar in attenuative properties to the eastern United States, and that the tectonic regions exhibit higher attenuation than the shield regions in the period range below 20 seconds. In the period range above 20 seconds the two regions have similar attenuation. The regionalization was found to lower the standard deviations considerably and to eliminate negative values obtained from some average attenuation coefficients determinations.

Fundamental-mode studies at high frequencies.

During this contract period, the effect which low-Q sediments have on surface wave amplitudes was investigated for the first time. Calculations showed that the fundamental Rayleigh mode at frequencies above 1 Hz were very quickly attenuated by layers of low-Q sediment (Q_β = 50) as thin as 50-100 meters. These calculations were supported by observations of high frequency fundamental-mode Rayleigh waves in southeastern Missouri and southern Illinois.

Higher-mode studies.

Regional studies of Q structure. A new method, employing the superposition of higher Rayleigh modes, as well as the fundamental mode was employed to study the Q structure of various tectonic provinces. The method is important because it can be used for single sources and single stations, thus permitting the investigation of anelasticity over much smaller regions than has previously been possible. The method has so far been applied to the Basin and Range province, the Colorado Plateau, the eastern United States and the Tibetan Plateau. Results have verified the previous model for the eastern United States obtained using fundamental-mode data. The upper crusts of the Colorado Plateau, and especially of the Basin and Range, were found to be characterized by lower Q values than the eastern United States. Preliminary results for the Tibetan Plateau suggest that Q values for the lower crust are lower than in any other continental region so far studied. Extensions of this work will continue over the next two years.

Synthetic seismogram calculations. Attempts were made to utilize synthetic Rayleigh wave seismograms to evaluate the effect of lateral complexities of crustal structure on surface waves. Calculations were performed utilizing normal mode theory and several higher modes, as well as the fundamental mode. Our calculations revealed that it was possible to compute synthetics which agreed reasonably well with the observations for paths across stable regions. It was not possible, however, to match synthetics to observations for paths through tectonic regions, or for paths from a source region in Novaya Zemlya. It was not possible with the data available to separate the effects of multi-pathing and complex near-source structure.

IV. Characteristics of earthquakes in subduction zones

Fault-motion in the Kurile Islands region.

The nature of subduction of the Pacific plate beneath the Kurile-Kamchatka island arc system was investigated through the study of focal mechanisms of larger earthquakes in that region. Fault-motion of normal-depth earthquakes is consistent with convergence of the oceanic plate in the direction N60°W with respect to the continental plate. Shallow earthquakes immediately beneath the trench are tensional in character, whereas those located seaward of the trench are compressional. Intermediate-depth earthquakes exhibit either axial compression or axial tension with respect to the plate. Deep-focus earthquakes in the Kuriles are compressional with respect to the axis of the descending plate. In the Hokkaido corner region, east-west striking normal faults and northward dipping tension axes in intermediate and deep-focus earthquakes imply hinge faulting and contortion of the Pacific plate between the steeply dipping Kurile Island segment of the plate and the more moderately dipping Japanese segment. The recurrence of earthquakes in the Tokachi-Oki region seaward of the Hokkaido corner indicates that the direction of convergence of the Pacific plate is unaffected by the presence of the junction of the two island arc systems.

Q structure above subduction zones.

Spectral ratios of pP and P phases were used to investigate the anelasticity of the region above the down-going portion of the Nazca plate. $\overline{Q}$ values for paths to stations in the United States were found to be lower, on average, and more erratic than those found for paths to eastern United States stations. Values of $\overline{Q}$ obtained from eastern United States stations are relatively low (300-400), suggesting passage of the waves through a low-velocity layer of considerable vertical extent between deep seismic sources ($\sim$ 600 km) and the lithosphere.

Complex earthquakes in southern Mexico.

A sequence of earthquakes occurred near the coast of Chiapas, Mexico commencing on April 29, 1970. The long-period P waveforms of the three most important events of this sequence were analyzed using synthetic seismograms. Although some perturbations in the wave forms are shown to be caused by near-source structure, others are produced by complexities in the earthquake source time-functions. The results show that the aftershock of April 30 at 0833 (M_S = 6.4) can be modelled by a simple point source with a seismic moment of 6.6 x 10^{25} dyne-cm. The foreshock of April 29 at 1122 (M_S = 6.3) consisted of two simple events 7 seconds apart having approximately the same seismic moment of 4.1 x 10^{25} dyne-cm. Four events were identified within the 15 second interval prior to the main rupture (M_S = 7.3) for which the seismic moment was 9.9 x 10^{26} dyne-cm. Apparently only two of those events are directly related to the main rupture process. Multiple event analysis indicates that a small faulted area and low rupture velocity seems to be characteristic of these earthquakes.

Strong attenuation of P-wave signals was observed over a certain range of distances and azimuths, especially at stations in the eastern United States. This can be produced either by effects due to the geometry of the plate or to very low Q values. The former explanation appears to be more likely.

The P-wave signatures of several other shallow and intermediate earthquakes in this region show that earthquakes occurring near the trench are characterized by complex P waveforms. This complexity is perhaps due to a heterogeneous distribution of stresses along the trench or to a heterogeneous plate composition. The interaction of the American plate with the Cocos and Caribbean plates possibly complicates the rupture mechanism of earthquakes in this area.

Research accomplished during the period April 1 - September 30, 1978

AMPLITUDES AND ATTENUATION OF SEISMIC CRUSTAL PHASES AT REGIONAL DISTANCES IN IRAN

by

Otto W. Nuttli

INTRODUCTION

Because of a high rate of seismicity in and on the borders of Iran and of the existence of three World-Wide Standardized Seismograph Network (WWSSN) stations in that country, the area is ideally suited for a study of the amplitudes and attenuation of seismic crustal phases.

Physiographically most of Iran is mountainous or of high-plateau character. An exception is the relatively small area to the west of the Zagros mountains, which consists of desert and the plains of the Tigris and Euphrates rivers. If crustal features correlate with physiography, the character of the Iranian crust can be expected to bear some similarity to that of the United States west of the Rocky mountains.

There are three WWSSN stations in Iran: Shiraz(SHI), Mashad(MSH) and Tabriz(TAB). Shiraz is in the southern part of the country, in the Zagros mountains (elevation 1595 meters). Mashad (elevation 999 meters) is in the northeast corner of the country, near the U.S.S.R. border. To the north of it is upland and plateau country, physiographically quite distinct from Iran. Tabriz is in the mountainous region of northwest Iran (elevation 1430 meters). For the present study film copies of the SHI and MSH seismograms were used, the former for the period January 1972 through September 1972 and the latter

for the period January 1972 through December 1974. Film copies of SHI and TAB seismograms for the years 1972 through 1974 are on order, but have not yet been received.

METHOD OF ANALYSIS

Because data for at most two stations were available for any individual earthquake, the usual procedure for determining attenuation, i.e., plotting amplitudes as a function of distance for a large number of stations covering a wide range of epicentral distances, could not be used. The procedure employed in this study was to equalize all amplitude data to an m_b=5.0 event, so that the data of all the events could be combined into a single attenuation curve for a particular seismic phase. Equalization was accomplished by multiplying observed ground amplitudes by the antilog of the difference between 5.0 and the m_b of the earthquake. This assumes that m_b is a measure of the ground amplitude at a period of 1 sec, and that the amplitudes of body and surface waves whose period is near 1 sec will scale directly as m_b.

The Lg amplitude data are fitted by theoretical attenuation curves of the form

$$A = A_o \exp(-\gamma\Delta)/\Delta^{1/3} (\sin \Delta)^{1/2} \qquad (1)$$

where γ is the coefficient of anelastic attenuation and Δ is the epicentral distance. Nuttli (1973, 1978) previously has used this equation to fit 1- and 10-Hz Lg amplitude data for the central and eastern United States. For the purpose of deriving magnitude formulas, the theoretical curves are approximated by straight-line segments on log A vs. log Δ graphs.

The attenuation of crustal body waves cannot be expressed by such a simple formula as Eq.(1). Accordingly, the data on a log A vs. log Δ graph are simply fitted by straight-line segments. This procedure yields formulas which can be

used either to determine m_b values or to estimate the level of ground amplitude of the crustal body waves at a distance Δ for an earthquake of a specified m_b value. The P-wave m_b formulas are valid also for ground motion from explosion-generated waves, but the S and Lg motion for explosions is expected to be less than that predicted by the earthquake-wave formulas. This reduction in amplitude of S and Lg waves relative to P waves for explosions can be used to discriminate explosions from earthquakes.

THE DATA

The regional catalogue of the International Seismological Centre (ISC) was searched to find earthquakes occurring in or on the borders of Iran for the three-year period 1972 through 1974. A list of earthquakes of m_b between 4.0 and 6.0 was compiled, and seismograms of all the earthquakes on this list were examined for suitable crustal phases. Ninety-four earthquakes were selected for study on this basis.

The epicentral coordinates of the ISC were used to determine distance to the stations. The m_b value given by ISC was used to equalize amplitudes to those of a 5.0 event. Although the m_b determinations are not error free, which will be reflected in the equalized amplitudes, it is likely that the errors are randomly distributed and simply will cause scatter in the amplitude data about mean curves. By restricting the earthquakes used to m_b values of 4.0 to 6.0, the error in equalized amplitudes should always be significantly less than an order of magnitude.

Figure 1 presents the amplitude data for the vertical component of the P wave. At distances of 200 km to approximately 500 km the P wave is Pn, and at larger distances it is a P wave refracted through the upper mantle. It is always the first wave arrival. Figure 1 shows that the amplitude of Pn at SHI is almost an

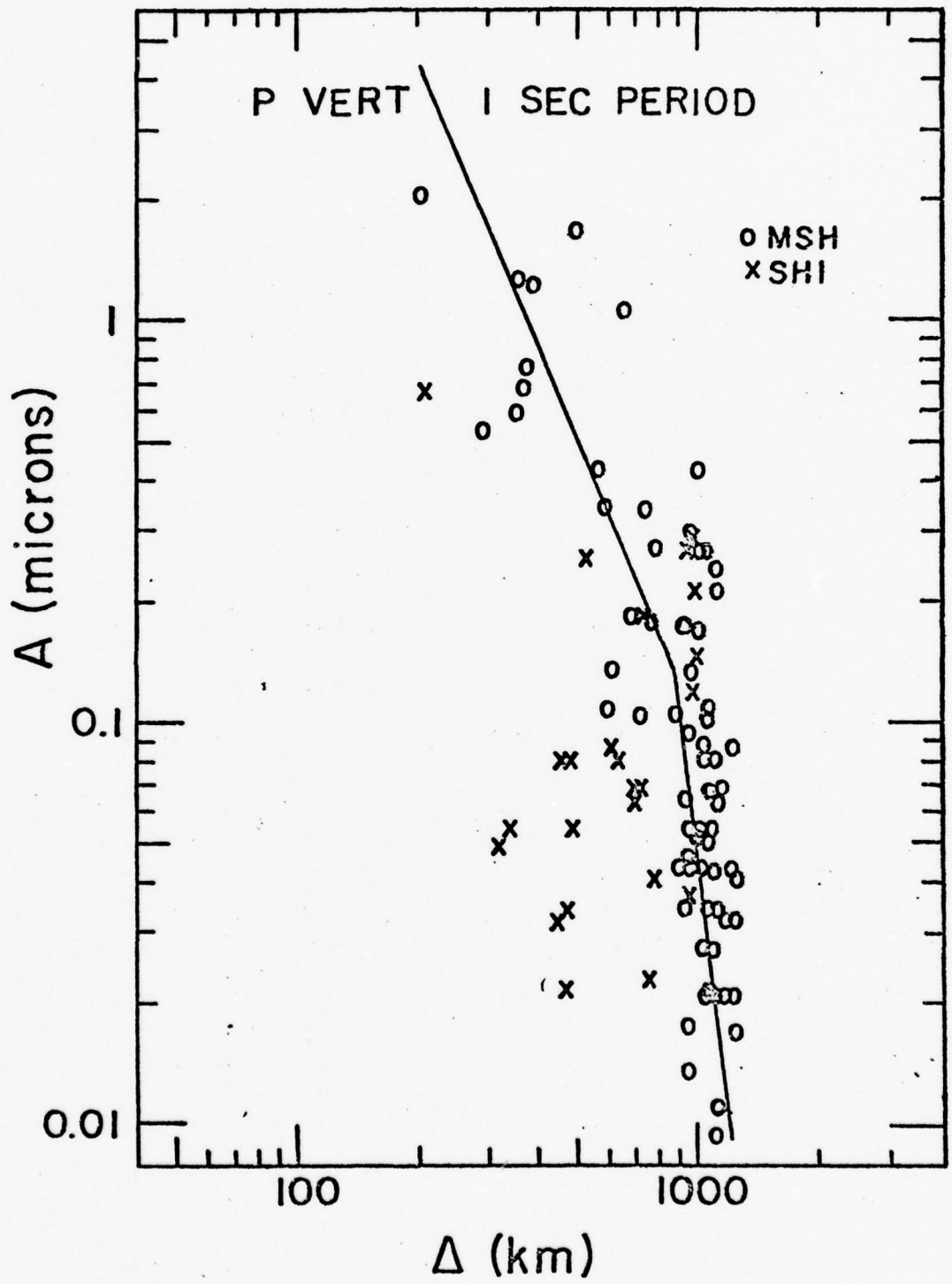

Figure 1. Amplitude of first P-wave arrival as a function of epicentral distance. The straight-line segments are approximations to the attenuation relation. The data are equalized to an m_b = 5.0 earthquake.

order of magnitude less than at MSH. At larger distances the P-wave amplitudes at the two stations do not show any appreciable differences. The scatter in the amplitude data of Figure 1 is great, equaling about an order of magnitude at most distances. The data can be represented by two straight-line segments. The first, from 200 to 900 km, represents the MSH, rather than the SHI, data. The second, from 900 to 1200 km, approximates the data of both stations.

Figure 2 gives the ground motion of the vertical component of the P* wave. As for the P wave, the amplitudes of the SHI motion are about an order of magnitude less than for MSH to distances of 500 km. As P* is not a distinctive phase on most seismograms, the number of data points is few. The data are approximated by two straight-line curves, one for distances of 200 to 700 km and the other for distances of 700 to 1100 km.

Ground motion for 1-Hz, vertical component Pg waves is shown in Figure 3. Once again for distances to 500 km the ground motion at SHI is about an order of magnitude less than at MSH. The data are approximated by two straight-line curves, one from 200 to 700 km and the other from 700 to 1200 km.

Figure 4 gives the 1-Hz, resultant horizontal component Sn ground motion. Although the number of data points is not large, they are fairly well represented by two line segments, from 170 to 850 km and from 850 to 1200 km.

Figure 5 presents the ground motion for the vertical component, 1-Hz Lg waves. The scatter in the data is not so great as for the P waves of Figures 1 to 3. The dashed lines are theoretical curves of the type given by Eq.(1), with $\gamma = 0.005$ and 0.004 km^{-1}. The straight-line segments are approximations to the theoretical curves, which will be used in deriving magnitude formulas. There are three segments, from 170 to 400 km, from 400 to 700 km, and from 700 to 1200 km.

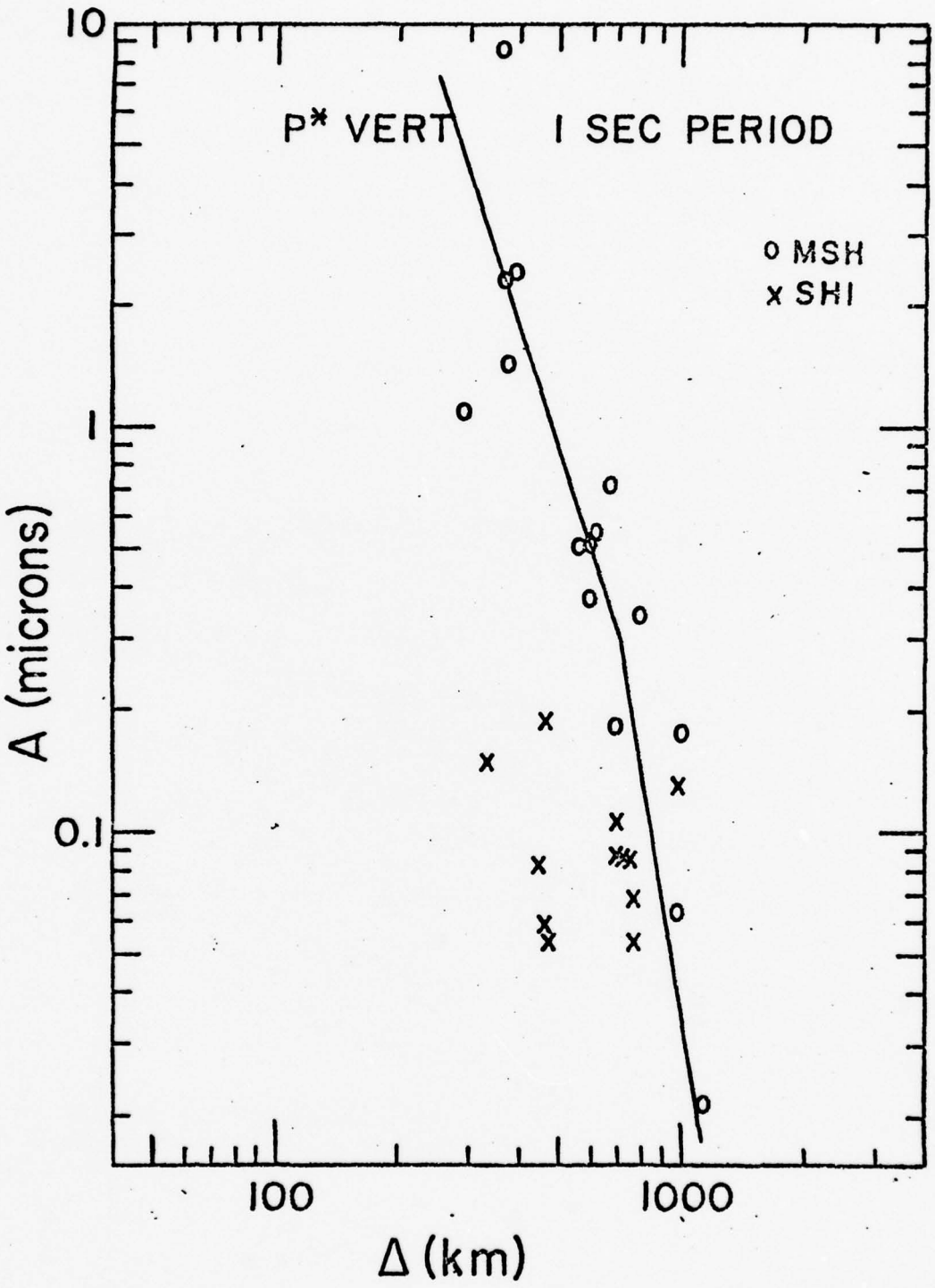

Figure 2. Amplitude of P^*-wave motion as a function of epicentral distance.

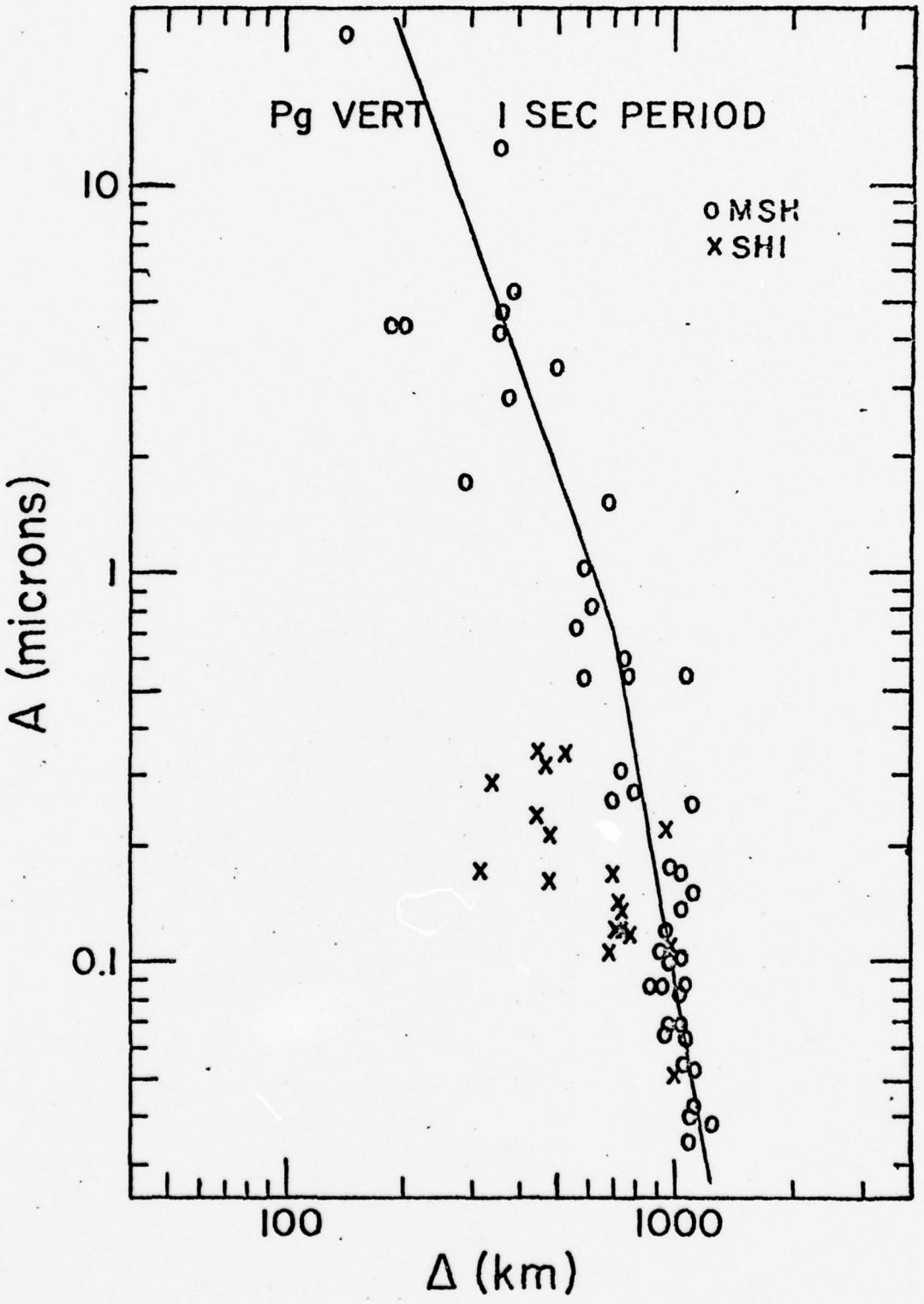

Figure 3. Amplitude of Pg-wave motion as a function of epicentral distance.

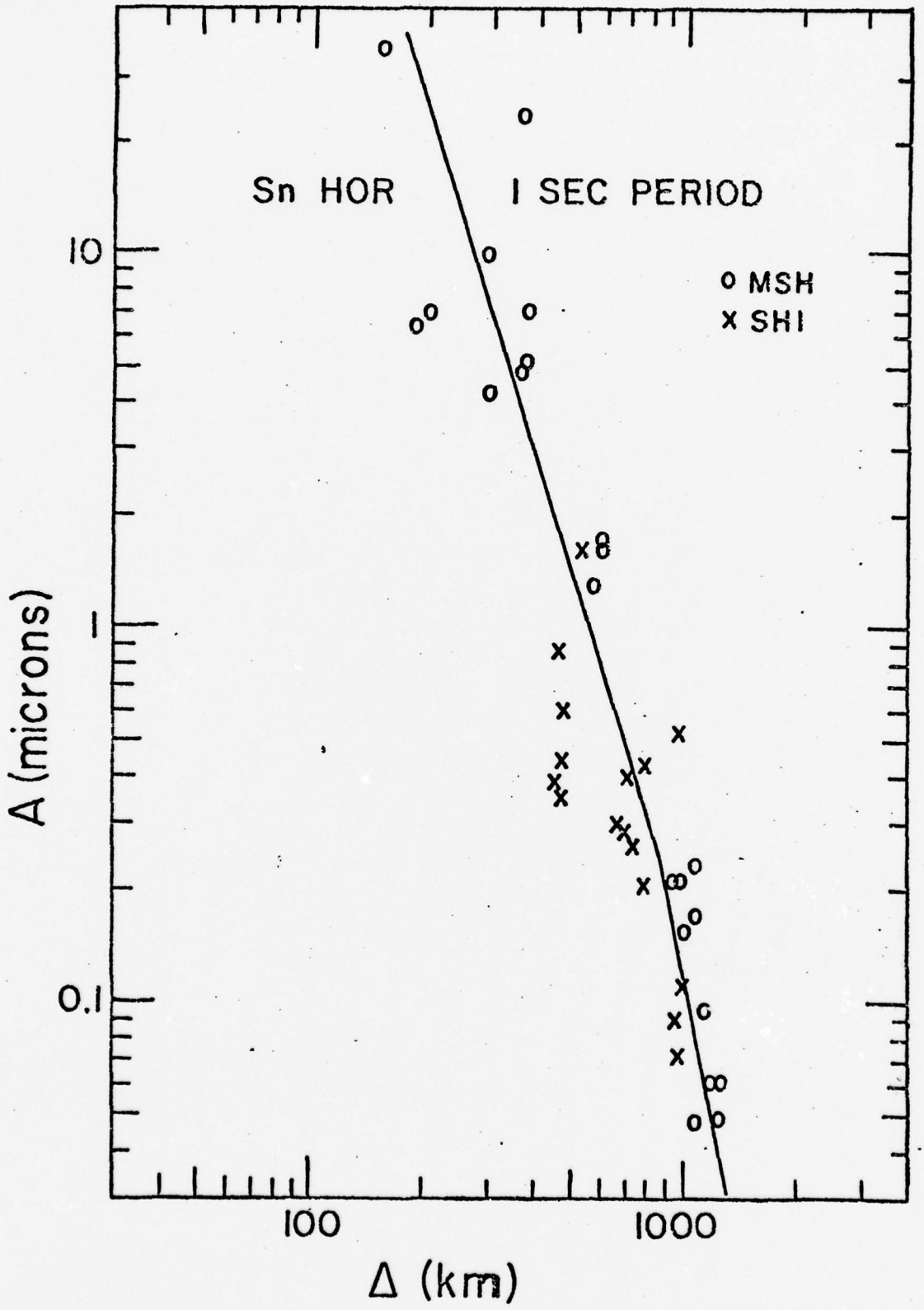

Figure 4. Amplitude of resultant horizontal Sn-wave motion as a function of epicentral distance.

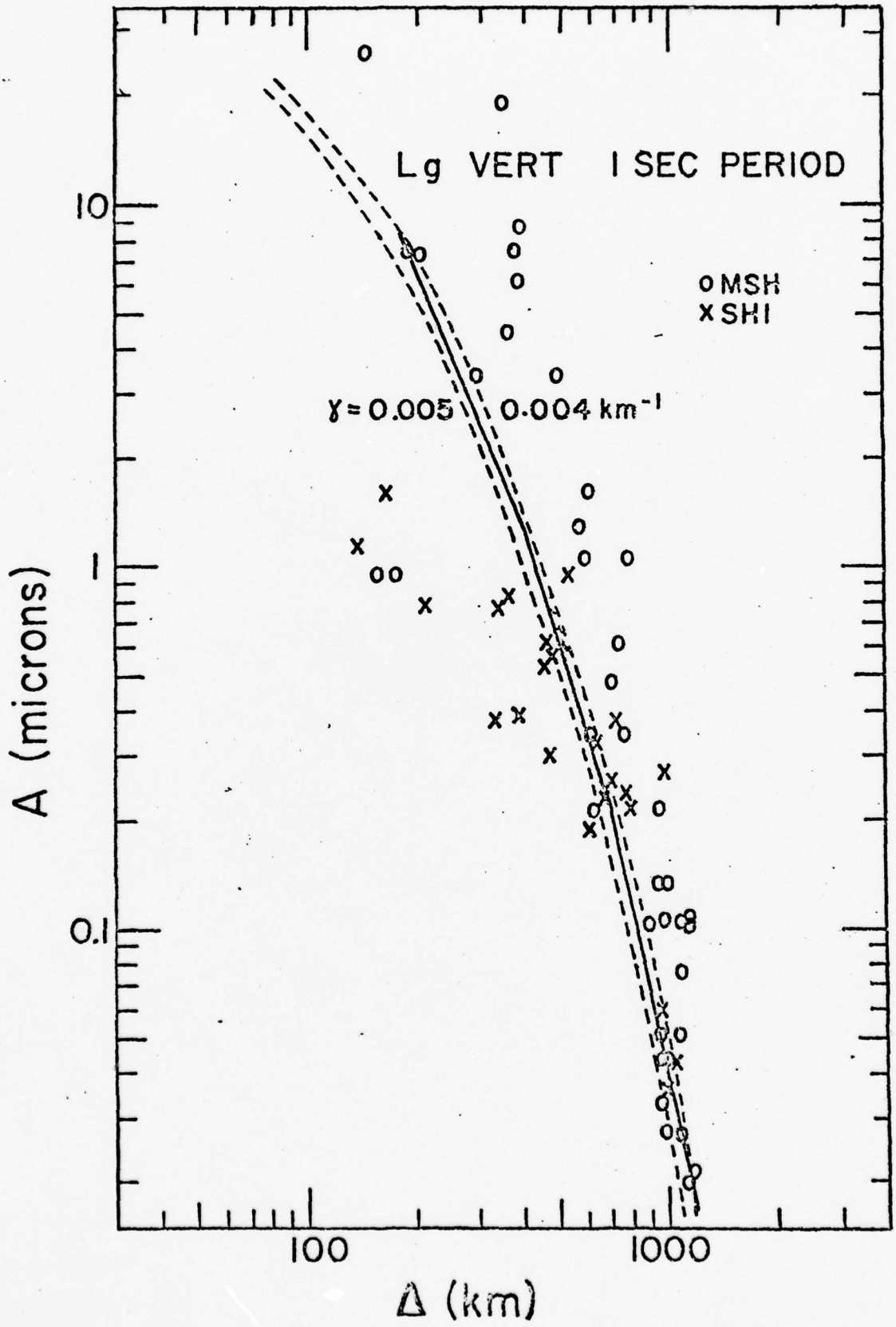

Figure 5. Amplitude of vertical component of 1-sec period Lg-wave motion as a function of epicentral distance. The dashed lines are theoretical attenuation curves. The solid-line curve is an approximation to the theoretical curves.

The 1-Hz, resultant horizontal component of the Lg motion is given in Figure 6. Data scatter is relatively small. Although the amplitudes are larger than those of the 1-Hz, vertical component Lg-wave motion, the data are fitted by similar curves with coefficients of anelastic attenuation of 0.005 to 0.004 km^{-1}. These curves are approximated by three straight-line segments at distances of 170 to 400 km, 400 to 700 km, and 700 to 1300 km.

All of the data of Figures 1 to 6 were obtained from short-period seismograms. These seismograms also showed prominent longer period surface waves, particularly at the larger distances. Amplitudes of the 3-sec period, vertical component wave motion were measured and plotted in Figure 7. To obtain data at distances of 500 km and less it was necessary to use long-period seismograms, because 3-sec period waves could not be recognized on short-period seismograms at these small distances. The coefficient of anelastic attenuation lies between 0.004 and 0.003 km^{-1}. The theoretical curves can be approximated by straight-line segments for distances of 200 to 800 km, and 800 to 1500 km.

MAGNITUDE FORMULAS

All of the data of Figures 1 to 7 were obtained by equalization to an $m_b = 5.0$ earthquake, and the straight-line segments which represent them are approximations to attenuation curves for an earthquake of that magnitude. Therefore, assuming that the relation

$$m_b = B + C \log \Delta + \log \Delta$$

applies to all the wave types shown in Figures 1 to 7, we can determine the values of the quantities B and C for each straight-line segment of each of the figures. For A in microns and Δ in kilometers, the resulting equations are:

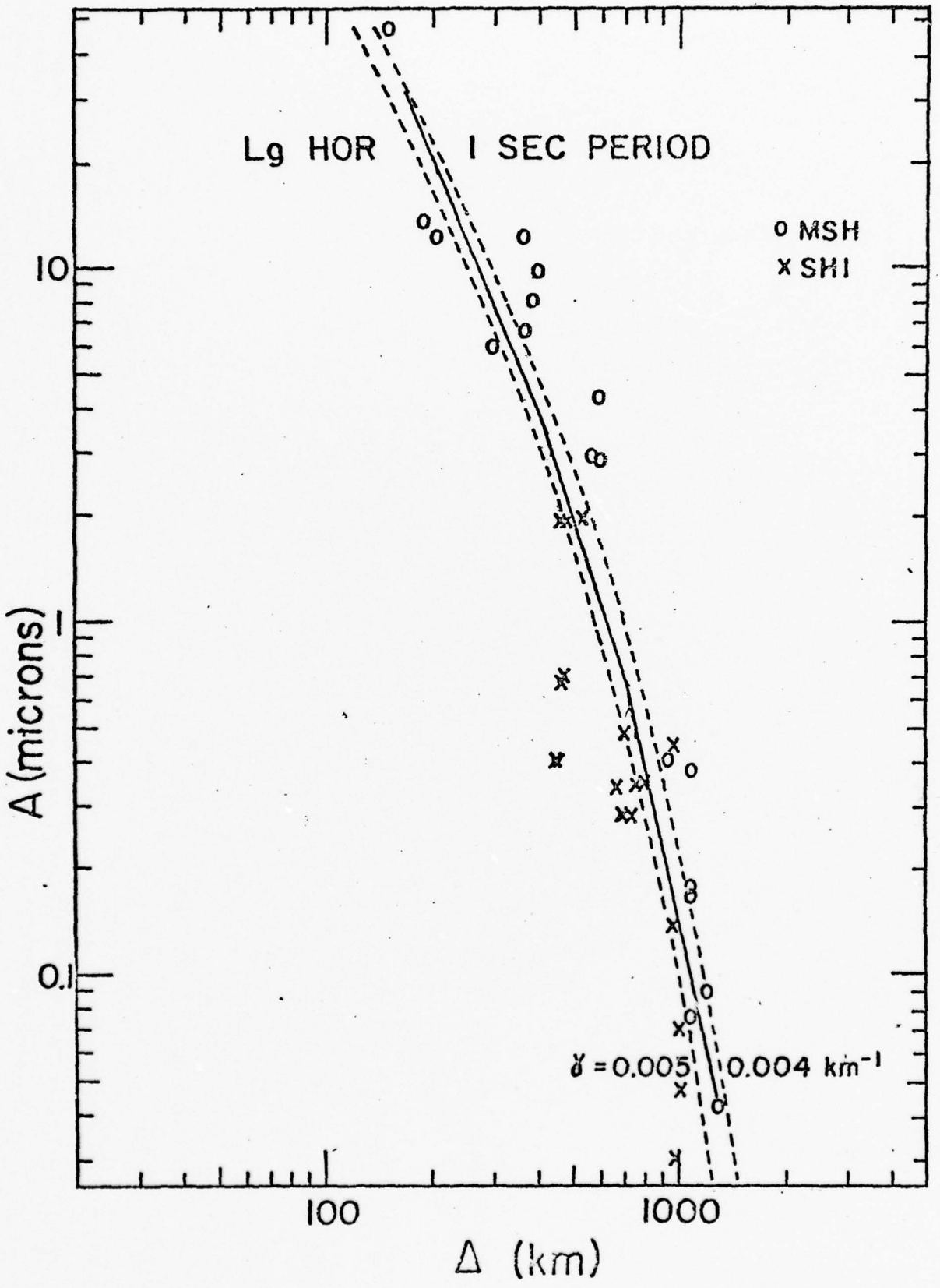

Figure 6. Amplitude of horizontal component of 1-sec period Lg-wave motion as a function of epicentral distance.

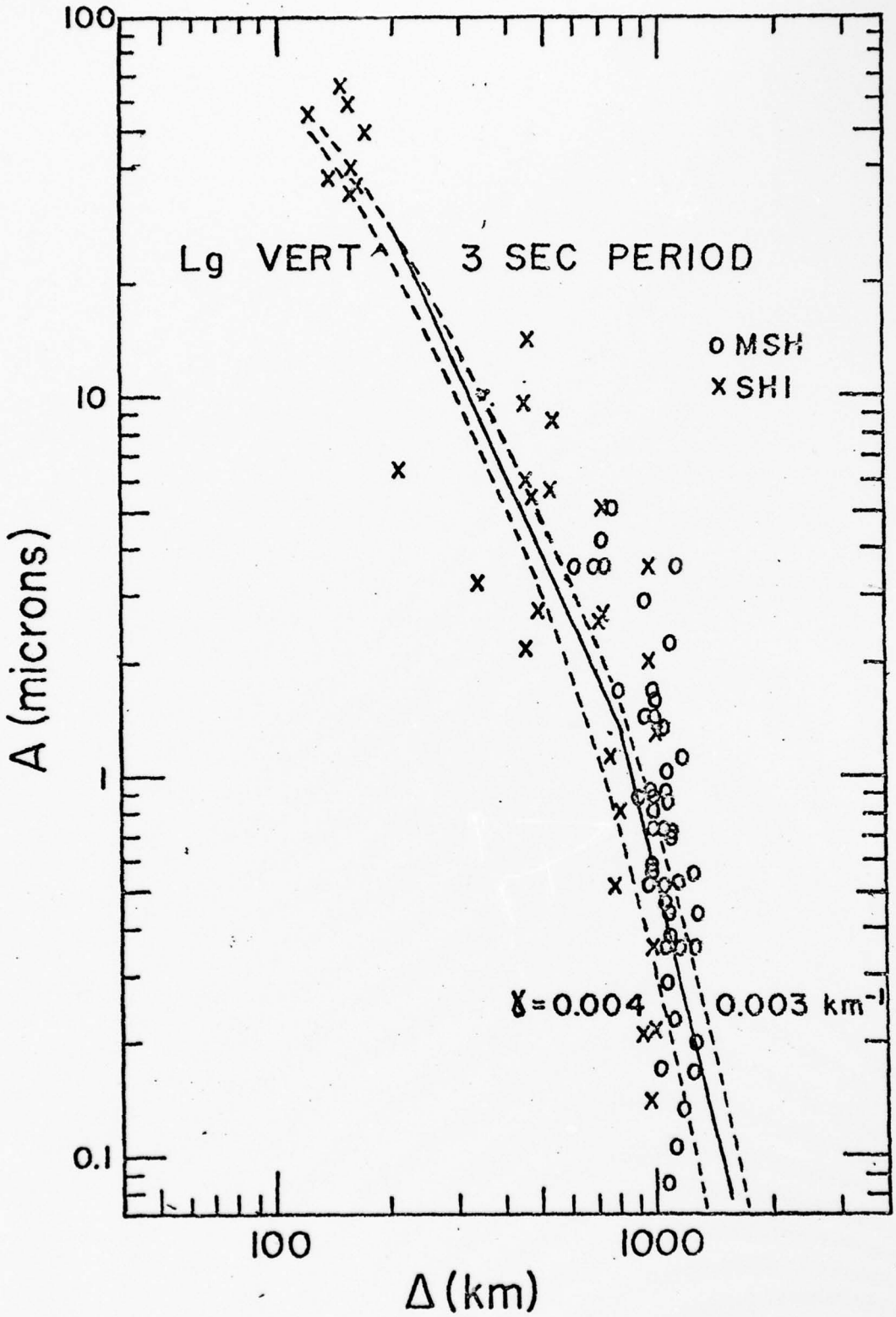

Figure 7. Amplitude of vertical component of 3-sec period Lg-wave motion as a function of epicentral distance.

For 1-Hz P waves, vertical component:

$$m_\Delta = -1.07 + 2.36 \log \Delta + \log A \quad \text{for } 200 \leq \Delta \leq 900 \text{ km}$$
$$m_b = -18.87 + 8.40 \log \Delta + \log A \quad \text{for } 900 \leq \Delta \leq 1200 \text{ km} \qquad (2)$$

For 1-Hz P* waves, vertical component:

$$m_b = -2.92 + 2.96 \log \Delta + \log A \quad \text{for } 200 \leq \Delta \leq 700 \text{ km}$$
$$m_b = -11.51 + 5.98 \log \Delta + \log A \quad \text{for } 700 \leq \Delta \leq 1100 \text{ km} \qquad (3)$$

For 1-Hz Pg waves, vertical component:

$$m_b = -2.72 + 2.76 \log \Delta + \log A \quad \text{for } 200 \leq \Delta \leq 700 \text{ km}$$
$$m_b = -11.40 + 5.85 \log \Delta + \log A \quad \text{for } 700 \leq \Delta \leq 1200 \text{ km} \qquad (4)$$

For 1-Hz Sn waves, resultant horizontal component:

$$m_b = -4.01 + 3.28 \log \Delta + \log A \quad \text{for } 170 \leq \Delta \leq 850 \text{ km}$$
$$m_b = -7.10 + 4.35 \log \Delta + \log A \quad \text{for } 850 \leq \Delta \leq 1200 \text{ km} \qquad (5)$$

For 1-Hz Lg waves, vertical component:

$$m_b = -1.40 + 2.42 \log \Delta + \log A \quad \text{for } 170 \leq \Delta \leq 400 \text{ km}$$
$$m_b = -3.36 + 3.18 \log \Delta + \log A \quad \text{for } 400 \leq \Delta \leq 700 \text{ km} \qquad (6)$$
$$m_b = -7.47 + 4.62 \log \Delta + \log A \quad \text{for } 700 \leq \Delta \leq 1200 \text{ km}$$

For 1-Hz Lg waves, resultant horizontal component:

$$m_b = -1.88 + 2.42 \log \Delta + \log A \quad \text{for } 170 \leq \Delta \leq 400 \text{ km}$$
$$m_b = -3.85 + 3.18 \log \Delta + \log A \quad \text{for } 400 \leq \Delta \leq 700 \text{ km} \qquad (7)$$
$$m_b = -7.96 + 4.62 \log \Delta + \log A \quad \text{for } 700 \leq \Delta \leq 1200 \text{ km}$$

For 3-sec period Lg waves, vertical component:

$$m_b = -1.50 + 2.20 \log \Delta + \log A \quad \text{for } 200 \leq \Delta \leq 800 \text{ km}$$
$$m_b = -7.80 + 4.35 \log \Delta + \log A \quad \text{for } 800 \leq \Delta \leq 1500 \text{ km} \qquad (8)$$

Eqs.(2) to (8) may be used to calculate body-wave magnitude if the amplitudes of one or more of the phases are available. Alternatively, they may be used to estimate ground motion for any of the phases considered for an earthquake of a given magnitude at a selected epicentral distance.

Eqs.(2) to (4) probably will overestimate the amplitude of the crustal P phases at SHI by as much as an order of magnitude to distances out to 500 km. Correspondingly at these small distances they will tend to underestimate m_b by as much as one unit if only SHI data are used.

DISCUSSIONS AND CONCLUSIONS

Figure 8 compares the amplitude levels of the crustal body phases for propagation through Iran. From the figure it can be seen that the Pg wave has the largest amplitude, and thus will in general be best suited for determination of body-wave magnitude of small events. Sn amplitudes are not much smaller than Pg amplitudes. Thus Sn can also be used for magnitude determination if data from horizontal component instruments are available. P* is often difficult to identify, and its amplitude falls off rapidly at distances beyond 800 km. Therefore, it is not very useful for magnitude determinations.

The first P arrival, which is Pn from distances of 200 to about 500 km and a wave refracted through the upper mantle at larger distances, has the smallest amplitude. Thus it is least suited for magnitude determinations of small events. However, it is the only phase of all the crustal waves whose onset time can be accurately determined. Therefore, it is the best and only wave to be used for location of Iranian events. In contrast to the western United States, where the onset of Pg is sharp, and the eastern United States, where the onset of Lg is clear, the Iranian crustal phases, except the first P arrival, all have emergent and indefinite beginnings.

Figure 9 shows the amplitude relations for the horizontal and vertical component of the 1-Hz Lg wave and for the vertical component of the 3-sec period Lg wave. The 1-Hz, horizontal Lg amplitudes are about three times those

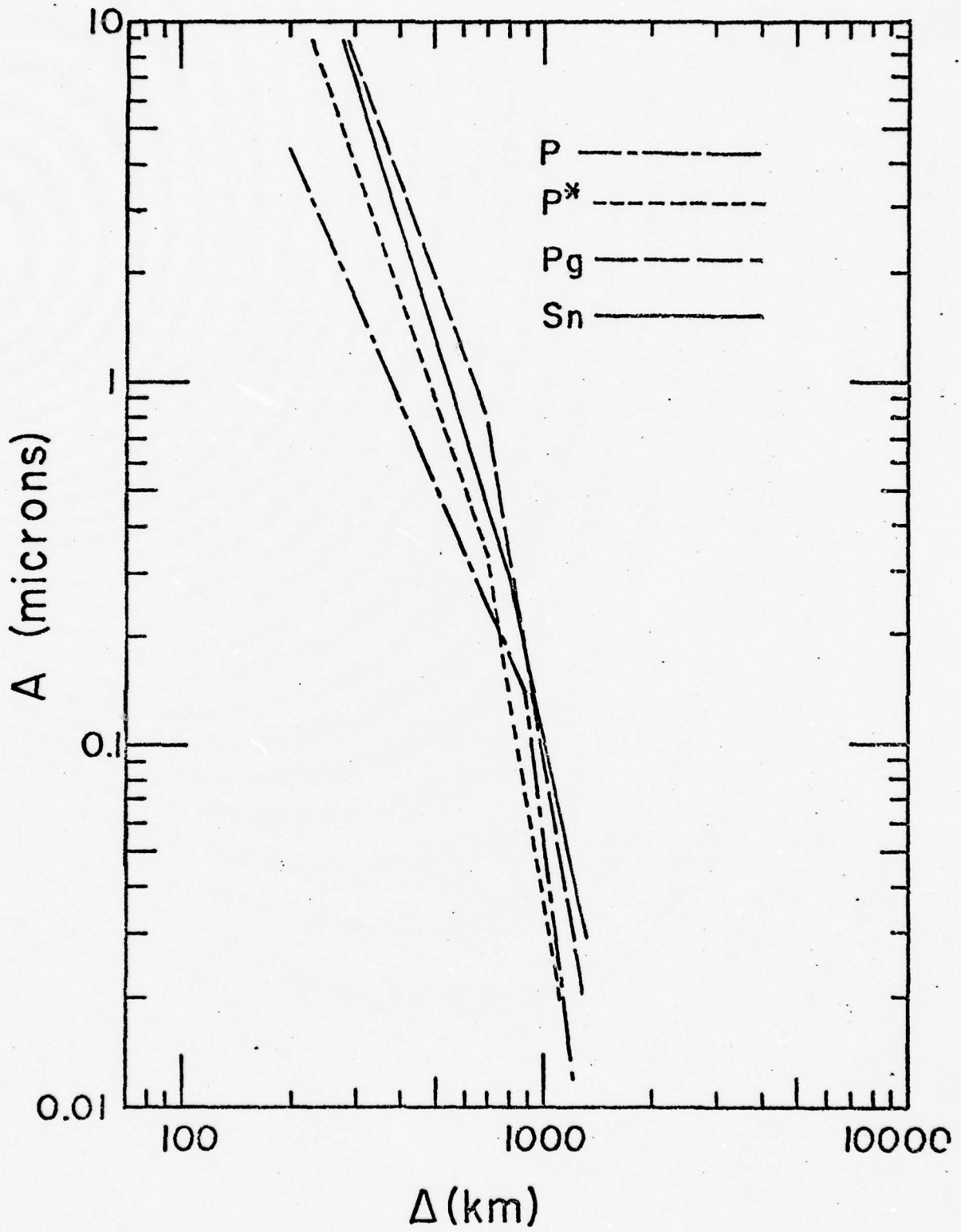

Figure 8. Comparison of amplitudes of 1-sec period body waves in Iran for an m_b = 5.0 earthquake.

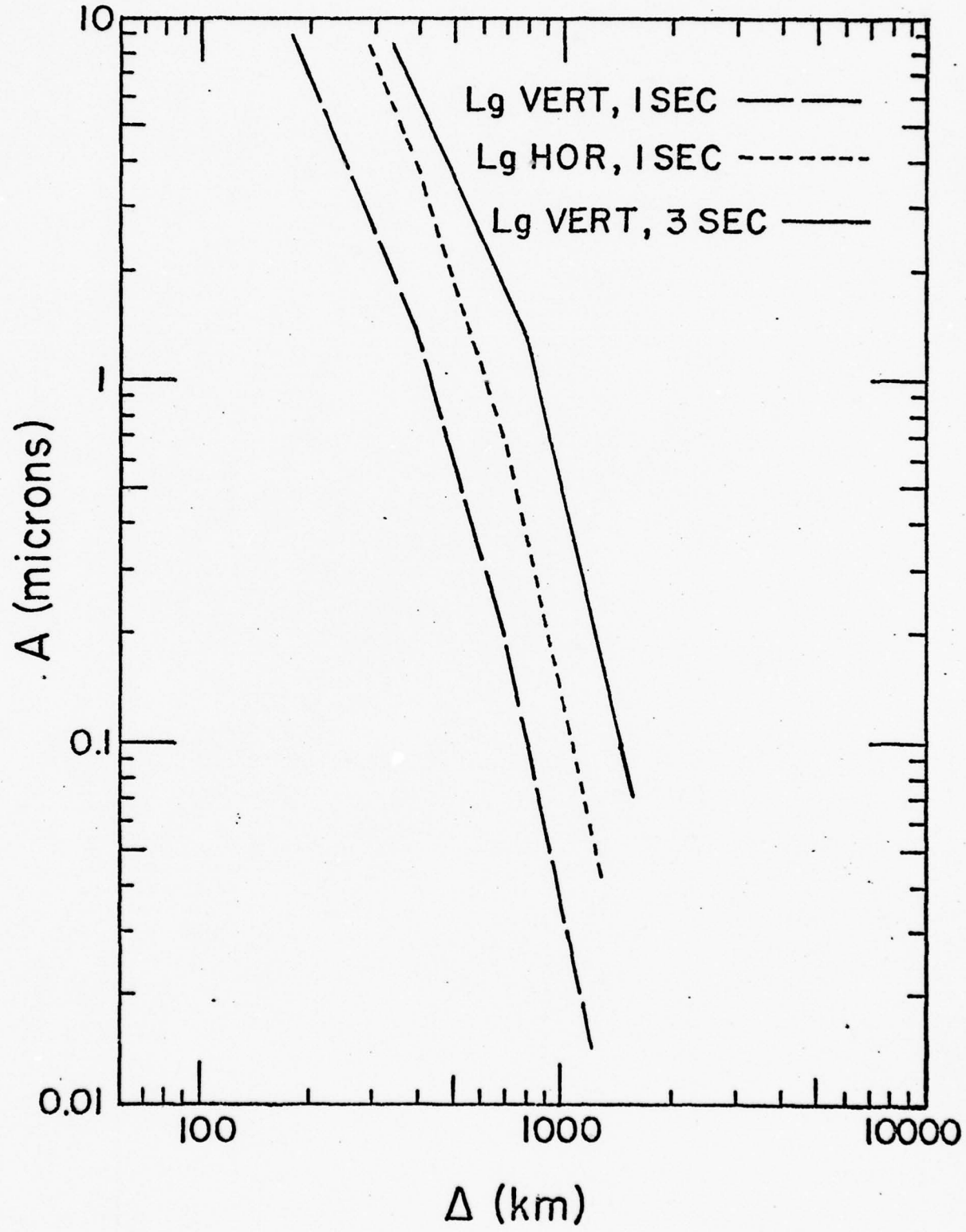

Figure 9. Comparison of Lg-wave amplitudes for an m_b = 5.0 earthquake.

of the vertical component of the 1-Hz Lg wave, and are about equal in amplitude to the vertical component of the 1-Hz Pg wave. At distances less than 500 km the 3-sec, vertical component Lg amplitudes are about five times greater than for the 1-sec, vertical component amplitudes. The difference between their amplitudes gets greater at larger distances, because the coefficient of anelastic attenuation is less for 3-sec than for 1-sec waves. The excitation, or amplitude difference between 1- and 3-sec Lg waves, will change with magnitude as the corner period of the Lg spectrum changes. For smaller events, where the corner period is 1 sec or less, the amplitudes of 1- and 3-sec Lg waves are expected to be the same as distances out to about 500 km, although the 1-sec amplitudes will be less at large distances because of differences in anelastic attenuation.

Knowing the value of the coefficient of anelastic attenuation and the group velocity of Lg waves, one can compute an apparent Q for these waves by means of the formula

$$Q = \pi f/\gamma U$$

where f is wave frequency, γ is the coefficient of anelastic attenuation and U is the group velocity. Using $\gamma = 0.0045$ km^{-1} and U = 3.5 km/sec for 1-Hz waves, this gives an apparent Q of 200, similar to what is observed in California for 1-Hz Lg waves. Nuttli and Dwyer (1978) have shown that the apparent Q of Lg is constant in the central United States for frequencies of 1 to 10 Hz. If the same holds true in Iran, the coefficient of anelastic attenuation for 10-Hz Lg waves would be 0.045 km^{-1}. Figures 10 and 11 compare the attenuation of 1- and 10-Hz Lg waves, respectively, for the central United States and Iran. Although we do not yet have any seismological data to support such a conclusion, from similarities in crustal geology between Soviet Asia and the central United States we might expect the area of the U.S.S.R. north and to the east of Iran to have

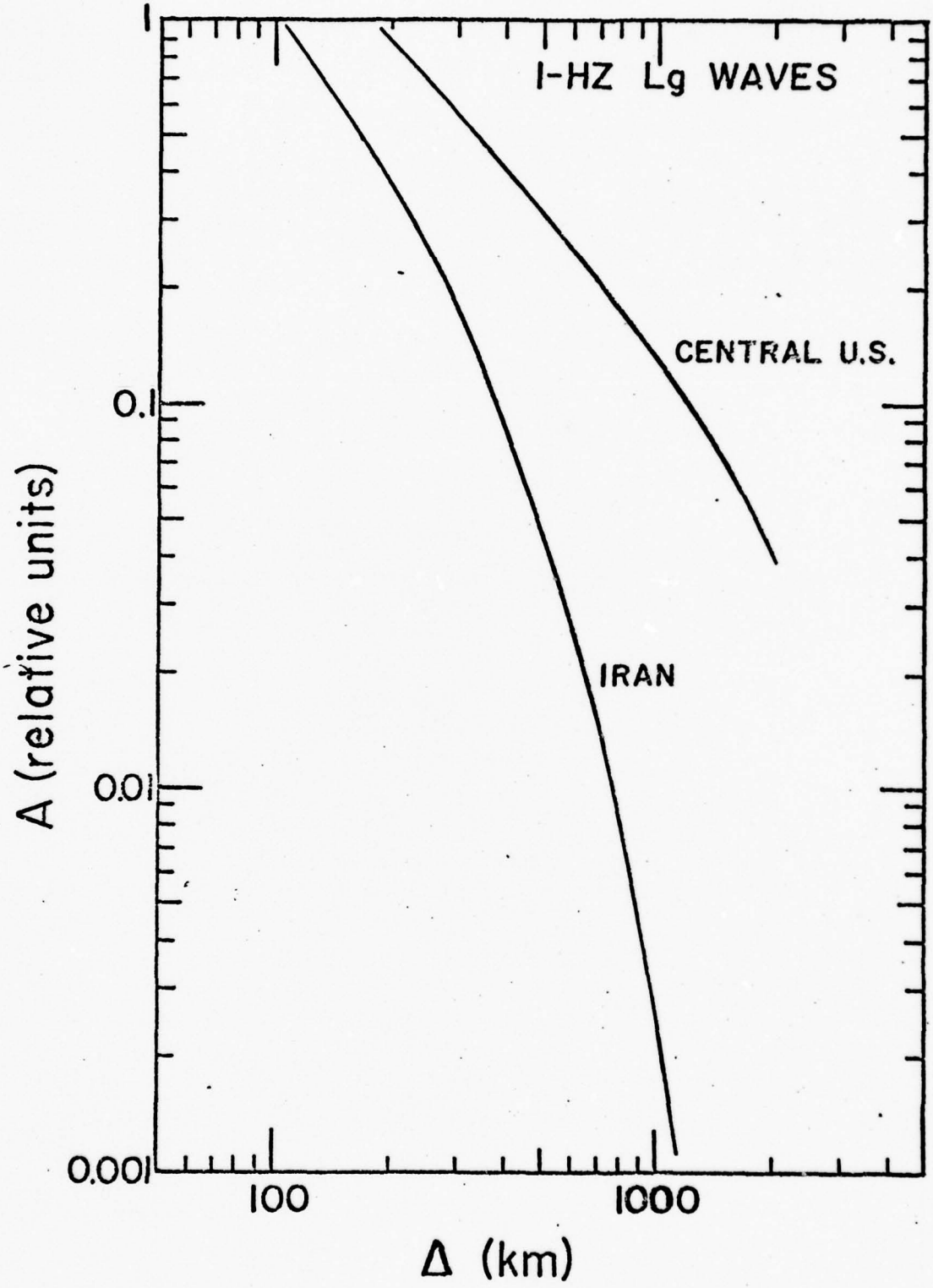

Figure 10. Comparison of 1-Hz Lg-wave attenuation in the central United States to that in Iran.

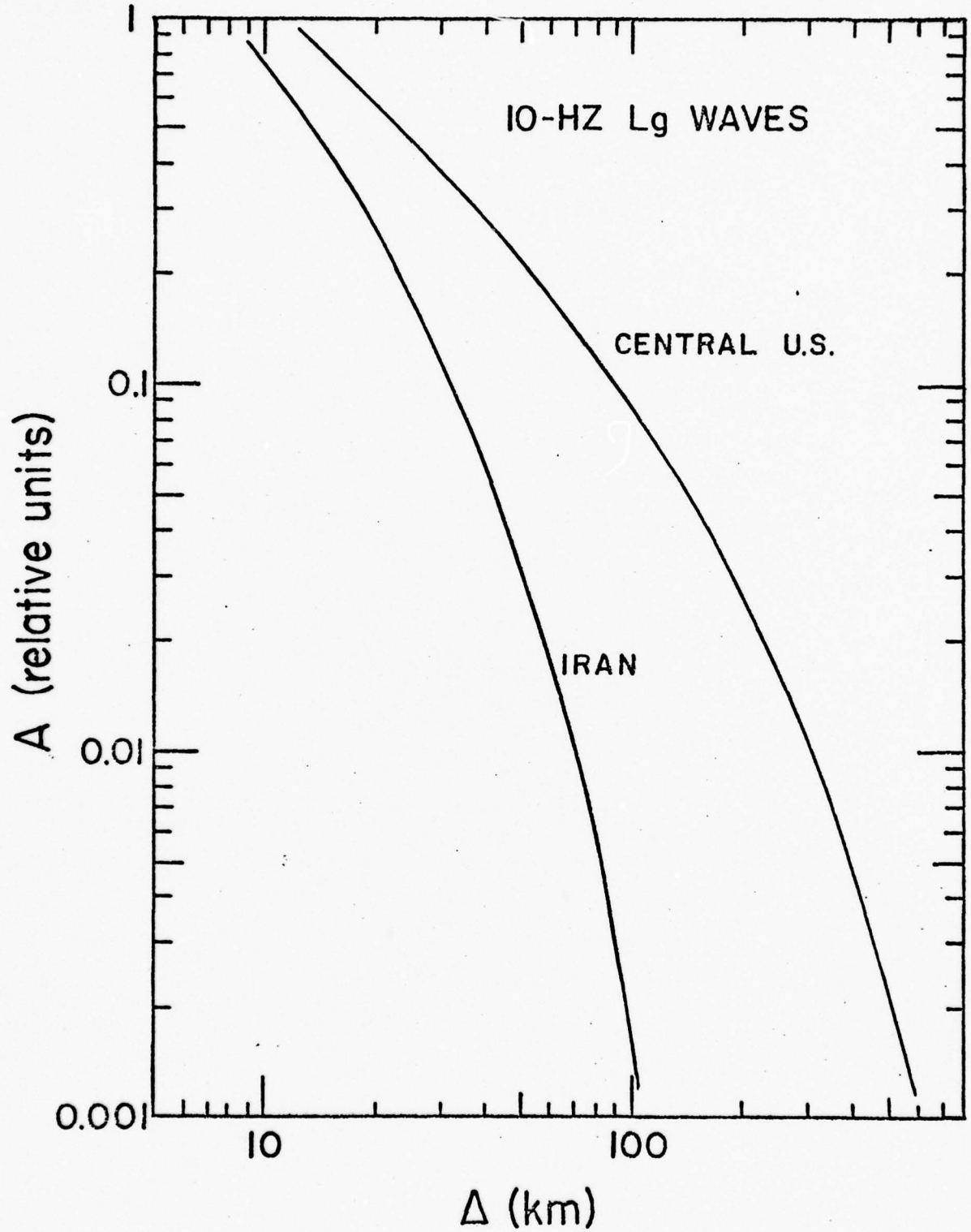

Figure 11. Comparison of 10-Hz Lg-wave attenuation in the central United States to that in Iran. The Iranian curve is hypothetical, rather than based on actual 10-Hz data, and assumes an apparent Q value of 200 for 10-Hz waves.

Lg attenuation similar to the central United States. Assuming the same source excitation for a given magnitude event, from Figure 10 we can see that 1-Hz Lg waves in the central United States will have six times the amplitude of those in Iran at 500 km distance. The difference increases to over fifty times at a distance of 1000 km. From Figure 11 it can be seen that 10-Hz Lg waves in the central United States have six times the amplitude of those in Iran at a distance of 50 km, and more than fifty times the amplitude at a distance of 100 km. Roughly speaking, we can say that 10-Hz Lg waves will propagate as efficiently in the central United States as 1-Hz Lg waves propagate in Iran. In Iran 10-Hz Lg waves will die out at very short epicentral distances. All of the above statements are based on the assumption that apparent Q is constant in Iran for frequencies of 1 to 10 Hz, as is observed for the central United States.

No explosions occurred in Iran, so we are unable to compare the excitation of the crustal P waves to the crustal S and surface waves. It is expected that the crustal S and surface waves will have relatively low excitation for explosions, compared to earthquakes, and that this will serve as one way to discriminate between earthquakes and explosions. This point will be tested when we look at earthquakes in central Asia and explosions in Kazakhstan.

REFERENCES

Nuttli, O.W. (1973) "Seismic wave attenuation and magnitude relations for eastern North America", Journal of Geophysical Research, 78, 876-885.

Nuttli, O.W. (1978) "A time-domain study of the attenuation of 10-Hz waves in the New Madrid seismic zone", Bulletin of the Seismological Society of America, 68, 343-355.

Nuttli, O.W. and Dwyer, J.J. (1978) "Attenuation of high-frequency seismic waves in the central Mississippi valley", Report 10, State-of-the-Art for Assessing Earthquake Hazards in the United States, U.S. Army Engineer Waterways Experiment Station, Vicksburg, Mississippi.

Source Parameters of some Eurasian Earthquakes

by Huei-Yuin Wen Wang

In this semi-annual report, we determined earthquake source parameters from a study of the long-period teleseismic P-wave character, and using these parameters we attempted to generate surface waves.

The Haskell-Thomson layer matrix method (Haskell, 1964; Hudson, 1969) for computing far-field body wave amplitudes from shear dislocations was used to generate synthetic P waveforms. A point source double-couple without moment was assumed. The source parameters are searched until the amplitude and the shape of the theoretical P-wave signals fit those of the observed seismograms.

A Szechwan earthquake which occurred on May 10, 1974 at 19:25 GMT was considered in this study. Since there is little research on the velocity model of this area, we determined a model using different combinations of the Gutenberg continental model (Dorman, et al., 1960) and Chun and Yoshii's (1977) Tibetan Plateau velocity model. Table 1 gives our source crust and upper mantle model for the Szechwan earthquake.

The fundamental-mode Rayleigh-group velocities (denoted by Δ in Figure 1) obtained from our model have been compared with those observational values (denoted by X, in Figure 1) obtained for 6 paths to the stations NUR, SHI, STU, IST, TAB, and ATU, by using the multiple filter technique (Dziewonski, et al., 1969; Herrmann, 1973). These two curves match quite well for periods larger than 18 seconds. Unfortunately, because of higher-mode contamination, the observed dispersion curve does not give values for periods smaller than 18 seconds. Therefore, we cannot say that our model is good enough for the shorter period waves.

The source parameters used were 17.2 km depth, strike 195°, dip 56° to the west, slip 63.5°, average seismic moment 0.75×10^{25} dyne-cm, and a triangular

time function with a rise time of 0.5 seconds and fall-off of 0.5 seconds.

The focal depth of 17.2 km was calculated by the pP-P method. This result is in agreement with the value obtained by ISC (see last semi-annual report). The fault plane solution was obtained in the standard way, using the sign of the long period first arrival of the P-wave motion. One of the nodal planes agrees with Kim and Nuttli's (1977) fault plane solution for three Szechwan earthquakes in a foreshock-aftershock sequence which occurred on Aug. 16, 1971. The other, however, differs in strike by about 90°. We have used Kim and Nuttli's (1977) solution for calculating synthetic seismograms. Their observations are explainable by the geological features and agree with those by the Ch'entu Seismological Office (1975) of the People's Republic of China. We will attempt to improve our solution with more observations in a future study.

The source time function was taken as a trapezoid pulse with three time segments: δt_1, δt_2, and δt_3, representing the rise time, fault duration, and fall-off time, respectively, and an area numerically equal to the seismic moment M_o. $T/Q = 0.4$ is used for all stations (see previous report).

At this moment, we have tried 30 different types of source function. None of them give synthetic P waveforms which agree with the observed ones for most stations. Figure 2 shows the best source pulse we have found so far. Its spectrum is given in Figure 3. In Figure 4, the theoretical (left) and observed (right) P-wave seismograms for the first 50 seconds duration at some stations are displayed. The quality of the match varies from station to station. In general, although the amplitudes and P-wave durations do not match the observed ones, the shapes of the theoretical waveforms are somewhat similar to those of the observed ones.

Assuming this source pulse is representative of this earthquake, it can be applied to compute synthetic surface waves if we know intrinsic Q values and

anelastic attenuation coefficients. Q_β value of 150 to a depth of 16.25 km and a value of 300 at greater depth were tested in this study.

Figure 5 presents a comparison of theoretical surface waves (top) with observed seismograms (bottom). Particular attention is paid to the fundamental mode. The durations and shapes of the envelope of the observed waveforms are similar to those for the computed waveforms for the fundamental-mode. Figure 5 also tells us that the amplitudes of synthetic seismograms are smaller than those of observed seismograms. We can increase the computed amplitudes by increasing the seismic moment. The observed signals have larger duration than the computed signals, which might be due to multipathing and lateral refraction and propagation through regions of varying crustal properties.

Discussion

Although the Haskell-Thomson matrix methods give a mathematically correct solution, they do not permit a direct interpretation of the origin of the phases shown on the theoretical seismograms (Langston, 1976). This makes it difficult to match P waveforms by this method.

Because the anelastic attenuation coefficients used represent a regional average rather than a value characteristic of a particular path, and because of the complexity of the structure and long propagation paths, different attenuation coefficients as well as different velocity models should be tested.

As soon as the computed seismograms fit the observed seismograms at most stations, the seismic moment can be used as a single parameter to scale the Szechwan earthquake.

References

Characteristics of precursory anomalies of the magnitude 7.1 earthquake in Shaotung, Ch'entu Seismological Detachment, Seismological Office, Szechwan Revolutionary Committee, Earthquake Frontiers 2, 14-19, 1975.

Chun, K.Y., and T. Yoshii, Crustal structure of the Tibetan plateau: A surface-wave study by a moving window analysis, Bull. Seism. Soc. Am., 67, 735-750, 1977.

Dorman, J., M. Ewing, and J. Oliver, Study of shear velocity distribution in the upper mantle by mantle Rayleigh waves, Bull. Seism. Soc. Am., 50, 87-115, 1960.

Dziewonski, A.M., S. Bloch, and M. Landisman, A technique for the analysis of transient seismic signals, Bull. Seism. Soc. Am., 59, 427-444, 1969.

Haskell, N.A., Radiation pattern of surface waves from point sources in a multi-layered medium, Bull. Seism. Soc. Am., 54, 377-393, 1964.

Herrmann, R.B., Some aspects of band-pass filtering of surface waves, Bull. Seism. Soc. Am., 63, 663-671, 1973.

Hudson, J.A., A Quantatitative Evaluation of Seismic Signals at Teleseismic Distances. II. Body waves and Surface waves from an extended source, Geophys. J. Roy. Ast. Soc., 18, 353-370, 1969.

Kim, S.G., and O.W. Nuttli, Spectral and magnitude characteristics of anomalous Eurasian Earthquakes, Bull. Seism. Soc. Am., 67, 463-478, 1977.

Langston, C.A., A body wave synthesis for shallow earthquakes sources: Inversion for source and earth structure parameters, Ph.D. Dissertation, Calif. Inst. of Technol., 1976.

Table 1

Source crust and upper mantle model for Szechwan earthquake

thickness (km)	p vel (km/sec)	S vel (km/sec)	density (g/cm^3)
3.5	4.50	2.60	2.40
15.5	5.98	3.40	2.74
19.0	6.32	3.65	2.80
30.0	6.75	3.90	2.90
	7.45	4.30	3.30

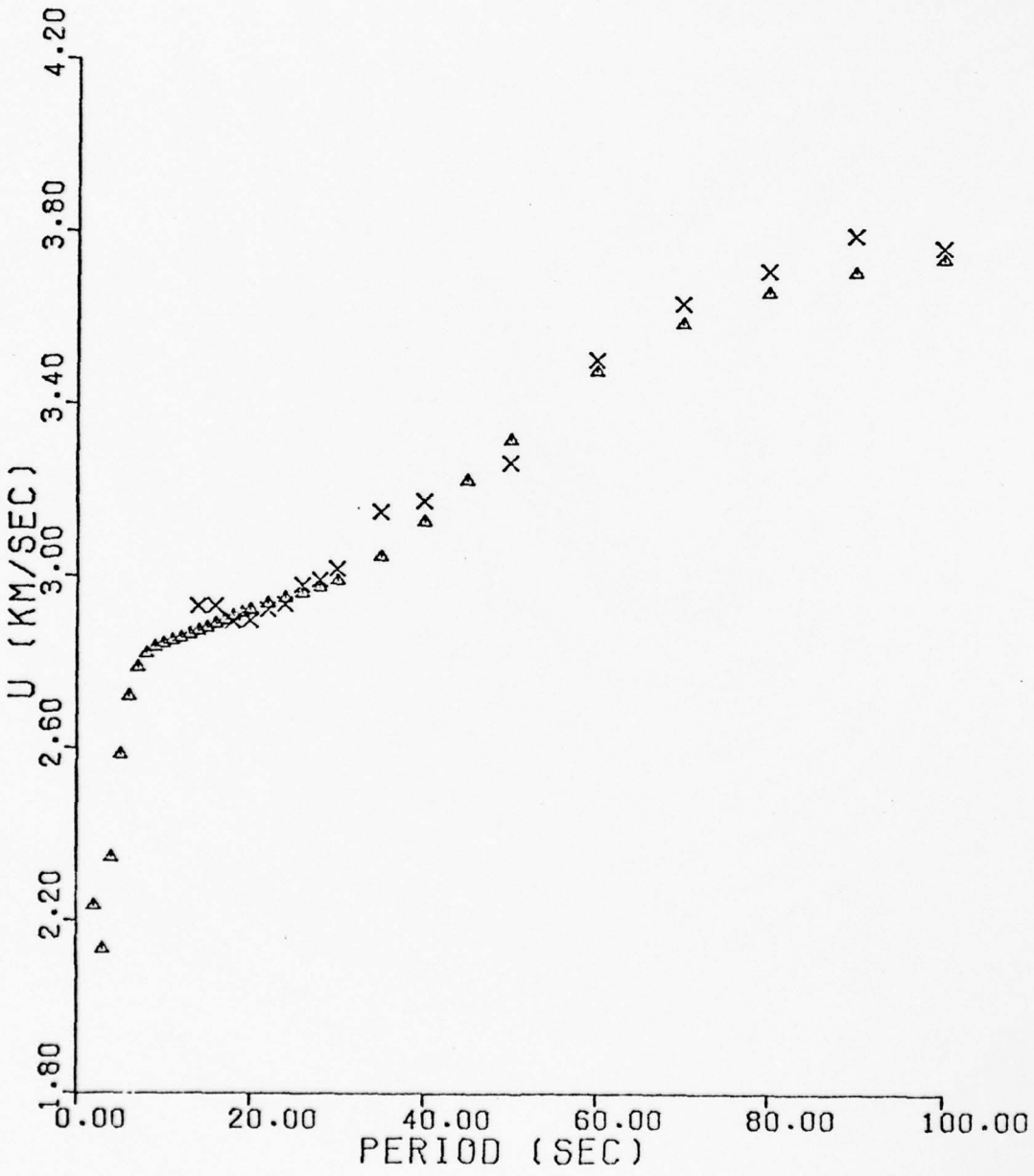

Figure 1. Fundamental-mode Rayleigh-group velocities for Szechwan Province.
Δ represents value from our model (Table 1),
X represents observational value obtained for 6 paths to the stations NUR, SHI, STU, IST, TAB, and ATU.

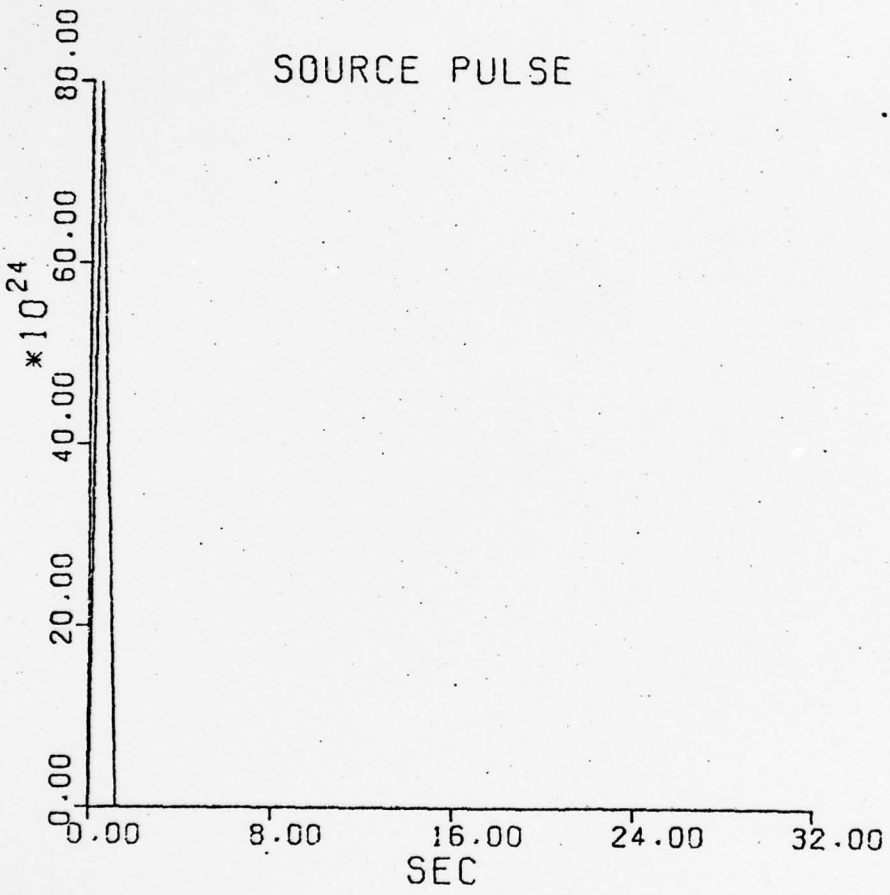

Figure 2. Source time function used for the Szechwan earthquake which occurred on May 10, 1974 at 19:25 GMT.

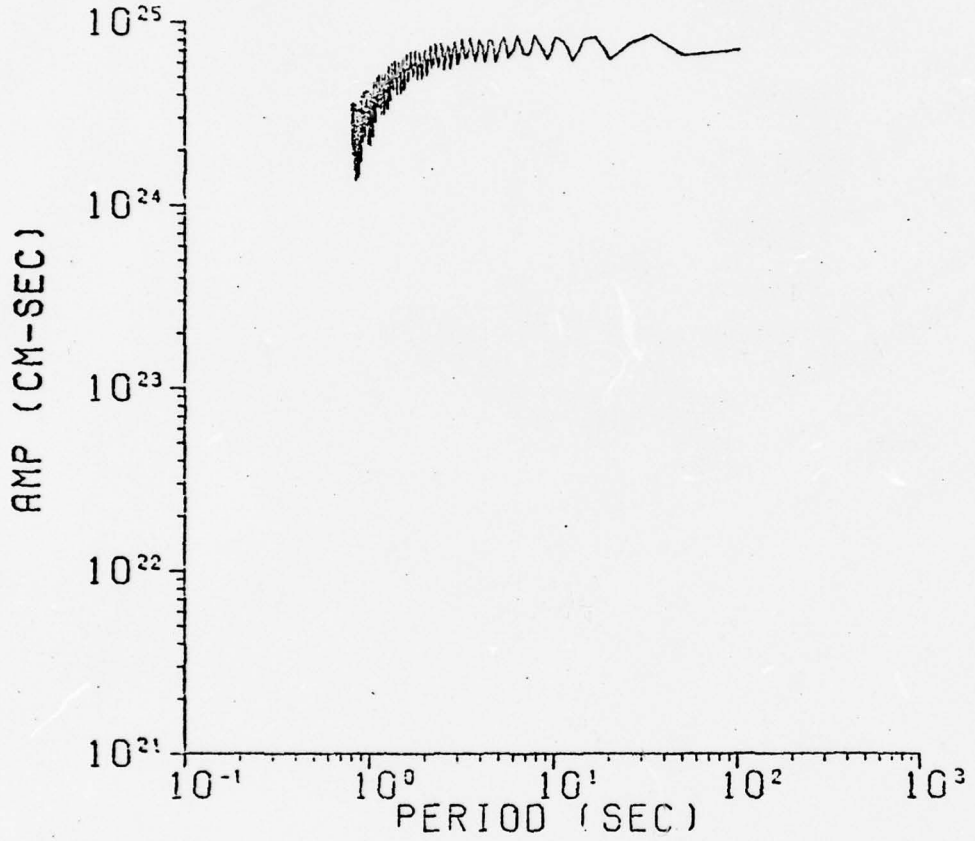

Figure 3. Source spectrum used for calculating the synthetic seismograms of the Szechwan earthquake which occurred on May 10, 1974 at 19:25 GMT.

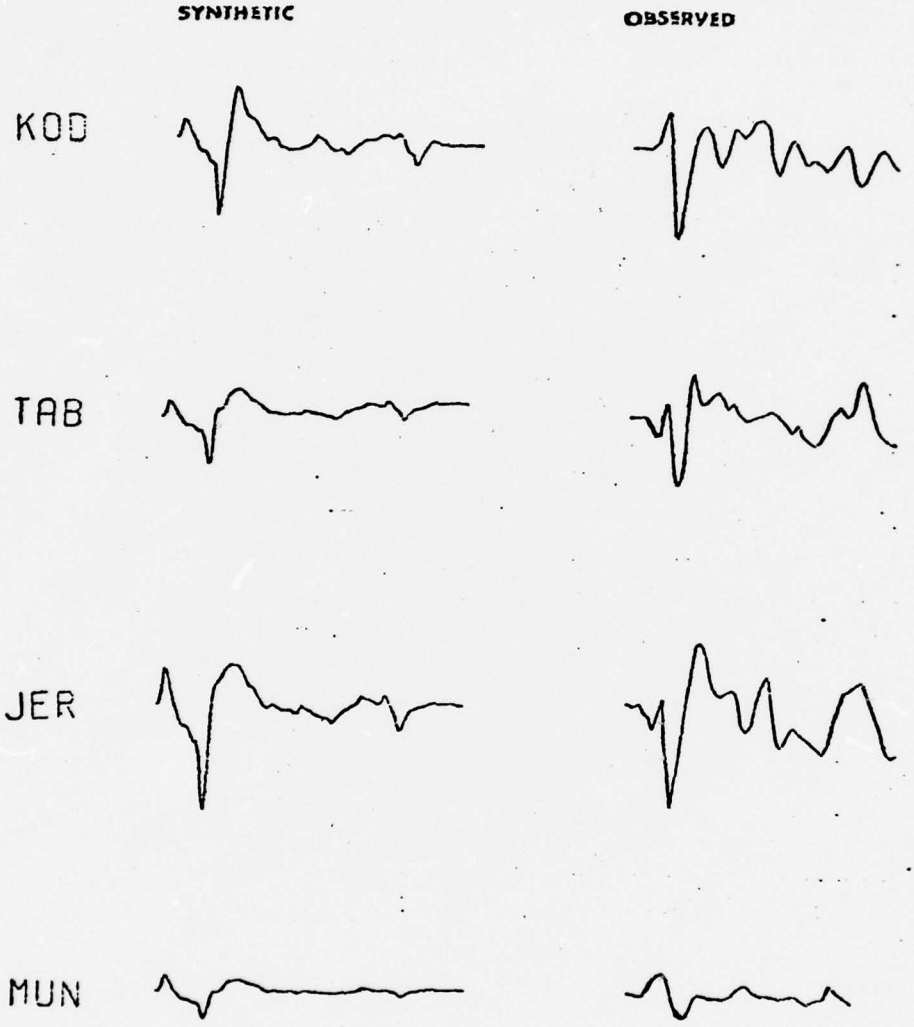

Figure 4

P-wave synthetic seismograms (left) and observed seismograms (right) for durations of 50 seconds at stations KOD, TAB, JER, and MUN.

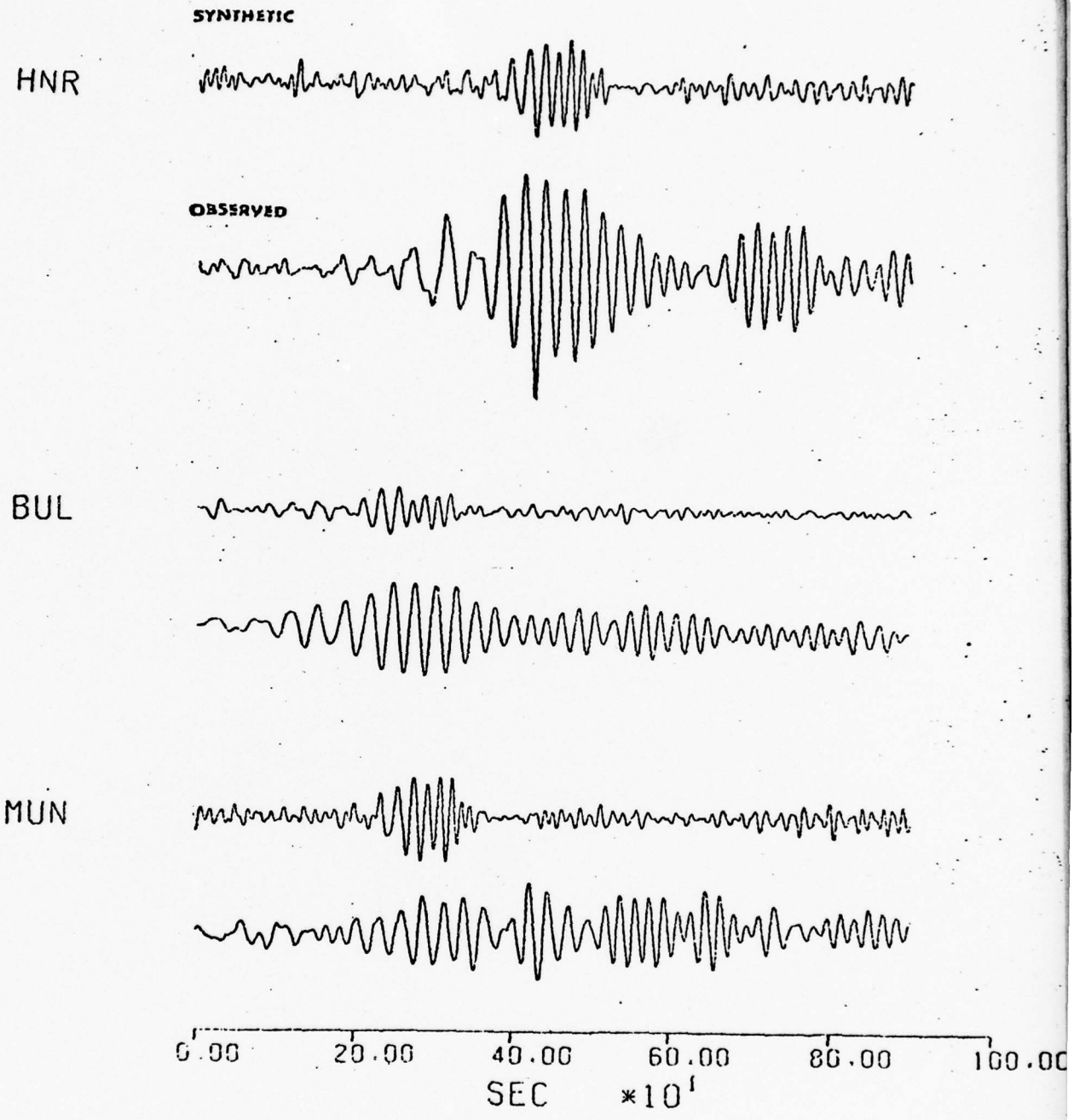

Figure 5

Rayleigh-wave synthetic seismograms (top) and observed seismograms (bottom) at stations HNR, BUL, and MUN.

Comparison and Inversion of Surface Wave Spectra

by Chiung-chuan Cheng

Rayleigh Wave Spectra Comparison for Eastern United States Paths

Our previous studies showed that comparison of observational and theoretical surface wave spectra could be applied in determining Q structures along wave paths. Comparisons for paths in the eastern United States have been made.

Figures 1, 2, and 3 show the spectrum comparisons for vertical component Rayleigh wave of the southeast Missouri earthquake of 21 Oct. 1965 recorded at stations ATL, GEO, and MDS. The simplified Q model obtained by Herrmann and Mitchell (1975), which has Q_β values of 250 from the surface to a depth of 17 km and values of 2000 at all greater depths, is used in computing the theoretical spectra.

The agreement in the comparisons is good for all the paths, except that some discrepancies can be noticed for the fundamental mode at very short periods.

Inversion of Surface Wave Spectrum

An inversion technique has been developed and tested in order to find the best fit between the observational and theoretical spectra.

Suppose that the observed surface wave spectral amplitude for a certain mode at a certain frequency is y_i. Let x_i be the corresponding theoretical amplitude computed from a Q model which has (N-1) layers overlying a half-space, with Q_β values being Q_j for j = 1, 2, --- N in each layer and the half-space respectively. Our objective is to find the particular combination of the seismic moment M, the focal depth h, and Q_β values which gives the best fit between x_i and y_i over all the observed frequencies and modes, assuming that

other factors involved in computing x_i are well determined.

Instead of matching x_i and y_i, we define

$$C_i = \log x_i$$
$$D_i = \log y_i$$

and the best fit is to minimize

$$\varepsilon^2 = \sum_{i=1}^{p} (C_i - D_i)^2$$

where p is the total number of observation data.

On the assumption that the source spectrum is $S(\omega) = \frac{M}{i\omega}$ and Q_α is twice the value of Q_β everywhere and Q_β is independent of frequency, the advantage of using C_i is that it is a function linear in log M and Q_j^{-1}'s, although still non-linearly dependent on h.

We can write

$$\log X_i = C_i (a_1, a_2, a_3, \ldots a_{N+2})$$

where $a_1 = \log M$, $a_2 = h$

and $a_{j+2} = Q_j^{-1}$, for j = 1, 2, --- N

Expanding C_i to first order in a Taylor's expansion,

$$C_i = C_{io} + \sum_{j=1}^{N+2} \left.\frac{\partial C_i}{\partial a_j}\right|_o \delta a_j$$

The subscript zero denotes that quantities are computed with initial values of M, h and Q_β model.

Minimizing ε^2 yields a set of N+2 simultaneous linear equations, which can be written as $A\alpha = \beta$ where A is a (N+2) x (N+2) matrix, and

$$A_{jk} = \sum_{i=1}^{p} \left.\frac{\partial C_i}{\partial a_j}\right|_o \left.\frac{\partial C_i}{\partial a_k}\right|_o$$

α and β are both (N+2) x 1 column vectors, and

$$\alpha_k = \delta a_k, \quad \beta_j = \sum_{i=1}^{p} (D_i - C_{io}) \frac{\partial C_i}{\partial a_j} \Big|_o$$

Using Marquardt's algorithm (e.g., Bevington, 1969) to solve for the parameter increment vector α, the matrix equation becomes $B\alpha = \beta$ where

$$B_{jk} = \begin{cases} A_{jk}\ (1 + \lambda) & \text{for } j = k \\ A_{jk} & \text{for } j \neq k \end{cases}$$

and λ is a constant factor.

The solution is obtained by

$$\alpha = B^{-1}\beta$$

A possible difficulty in using higher mode data is that each of these data has to be regarded as being associated with only a certain mode. The difficulty is solved by using only the arrival with the largest amplitude in the filtered wave train at each frequency. It is based on the fact that although, at a certain frequency, there might be waves of a few higher modes travelling with the same group velocity, their amplitudes differ among themselves. The largest amplitude is usually much larger than the others. Hence, it suffers only little interference in the wave train filtered for that frequency.

Figure 4 shows an example of theoretical Rayleigh wave spectra. The solid curves are the fundamental mode spectrum and the spectrum for the net result of the superposition of higher modes. The broken line represents the largest value of the amplitudes computed for individual higher modes.

To test the inversion technique, we assumed a Q model which had Q_1=100 in the 18 Km thick upper crust, Q_2=1000 in the 13 Km thick lower crust, and Q_3=2000 at all greater depths. The event was assumed to have the seismic moment of 3.2×10^{23} dyne-cm, and the focal depth of 18 Km. Theoretical Rayleigh wave

spectrum was computed for the net result of the fundamental and the higher modes. It was then filtered at various frequencies, simulating the procedure for actual observation. Twenty-one fundamental mode data and seventeen higher mode data were sampled, a total of p = 38. This data set of D_i's had a ε^2/p of 0.00153 compared to C_i's computed with exact M, h, and Q_j's. The inversion was started with M = 4.0×10^{23} dyne-cm, h = 10 Km, Q_1=200, and Q_2 and Q_3 being assumed known and not adjustable parameters. The inversion procedure was repeated until ε^2/p became stable. The results are shown in Table 1.

Another test was made with the same data, started with the same M, h and Q_1, but Q_2 and Q_3 both fixed at 500, a value lower than the true values. The results are shown in Table 2.

In both the tests, the inversion gave quite accurate focal depth and Q_1 after just a few iterations. The incorrectly assumed values for Q_2 and Q_3 in the second test did not affect the determination of the focal depth and Q1, but resulted in an incorrect seismic moment.

Rayleigh wave data from the GSC seismogram of the earthquake which occurred on 4 Oct. 1967 at 38.5 N, 112.1 W has been inverted. The starting parameters were those obtained in our previous study made with visual spectrum comparison. The Q model consists of an upper layer with a thickness of 18 Km overlying a half-space. Q_2 was fixed at 2000. The results of inversion are listed in Table 3. The spectra computed for the initial model and the final model are shown in figures 5 and 6 respectively.

Discussion and Conclusion

The spectrum comparisons made for paths in the eastern United States indicate that a model with a Q_β value of 250 in the upper crust provides an adequate fit to the data. In our previous report, the corresponding Q_β for

the western United States was found to be between 50 and 150. These results indicate that upper crustal Q_β values in the western United States are significantly lower than those for the upper crust of the eastern United States. The same conclusion was made by Mitchell (1975) using the fundamental Rayleigh mode.

The inversion of surface wave spectra enables us to find the parameters of the best fitting model in a systematic way without plotting spectra for intermediate models. Fixing Q_β in some deep layers at large values is usually helpful in preventing parameters from becoming negative after the inversion. Uncertainties in these presumed values might result in an incorrect seismic moment but would not adversely affect the determination of the focal depth and Q_β values at shallower depths.

References

Bevington, P.R., Data Reduction and Error Analysis for the Physical Sciences, McGraw-Hill, New York, 232-242, 1969.

Herrmann, R.B., and B.J. Mitchell, Statistical analysis and interpretation of surface-wave anelastic attenuation data for the stable interior of North America, Bull. Seism. Soc. Am., 65, 1115-1128, 1975.

Mitchell, B.J., Regional Rayleigh wave attenuation in North America, J. Geophys. Res., 81, 4904-4916, 1975.

Table 1
The First Test Inversion of Synthetic Data

Iteration	M ($\times 10^{23}$ dyne-cm)	h (Km)	Q_1	ε^2/p
0	4.000	10.000	200.000	0.07899
1	2.698	15.490	95.086	0.01861
2	3.139	17.991	107.689	0.00156
3	3.158	17.993	106.474	0.00153

Table 2
The Second Test Inversion of Synthetic Data

Iteration	M ($\times 10^{23}$ dyne-cm)	h (Km)	Q_1	ε^2/p
0	4.000	10.000	200.000	0.07791
1	2.707	15.659	98.807	0.02077
2	3.162	18.392	114.505	0.01954
3	4.395	18.144	109.540	0.00131
4	4.395	18.144	109.531	0.00131

Table 3
The Inversion of Data Observed at GSC

Iteration	M ($\times 10^{23}$ dyne-cm)	h (Km)	Q_1	ε^2/p
0	3.200	18.000	75.000	0.05422
1	6.717	18.508	46.657	0.03906
2	6.676	18.423	46.406	0.03861
3	6.639	18.345	46.186	0.03825
4	6.608	18.274	45.992	0.03797

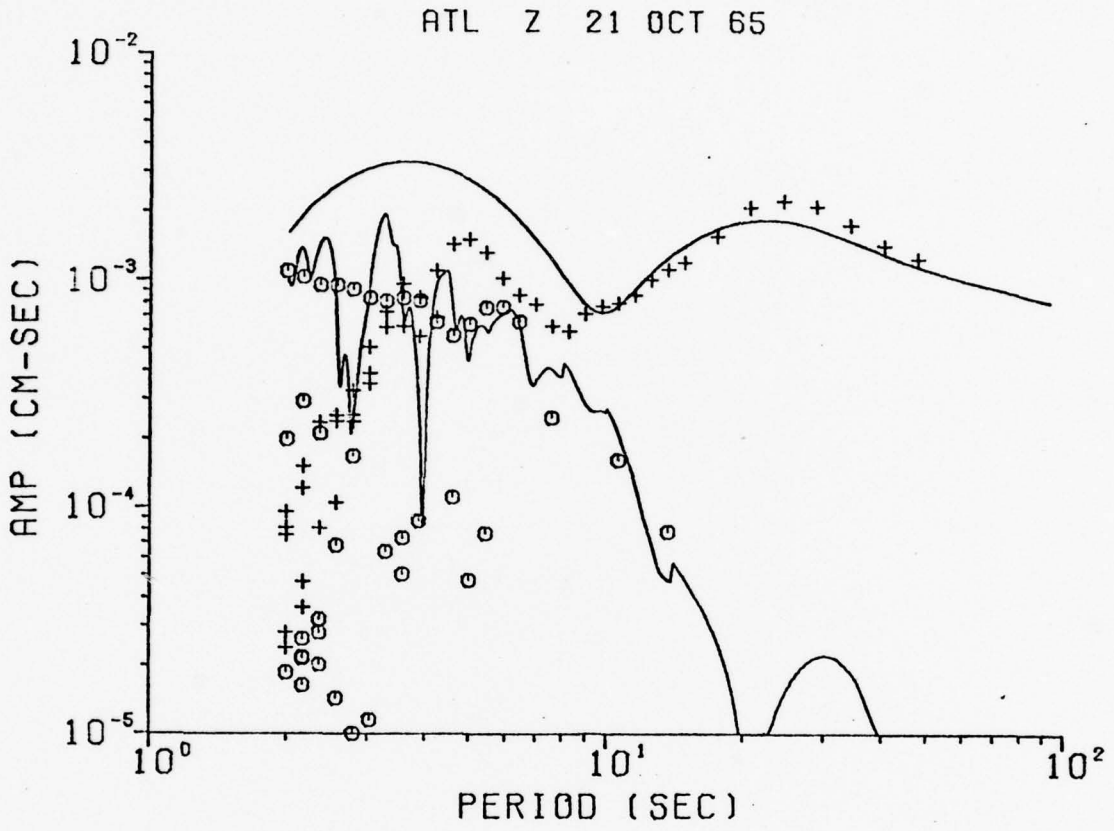

Figure 1. Comparison of theoretical and observational amplitude spectra for an eastern United States path.

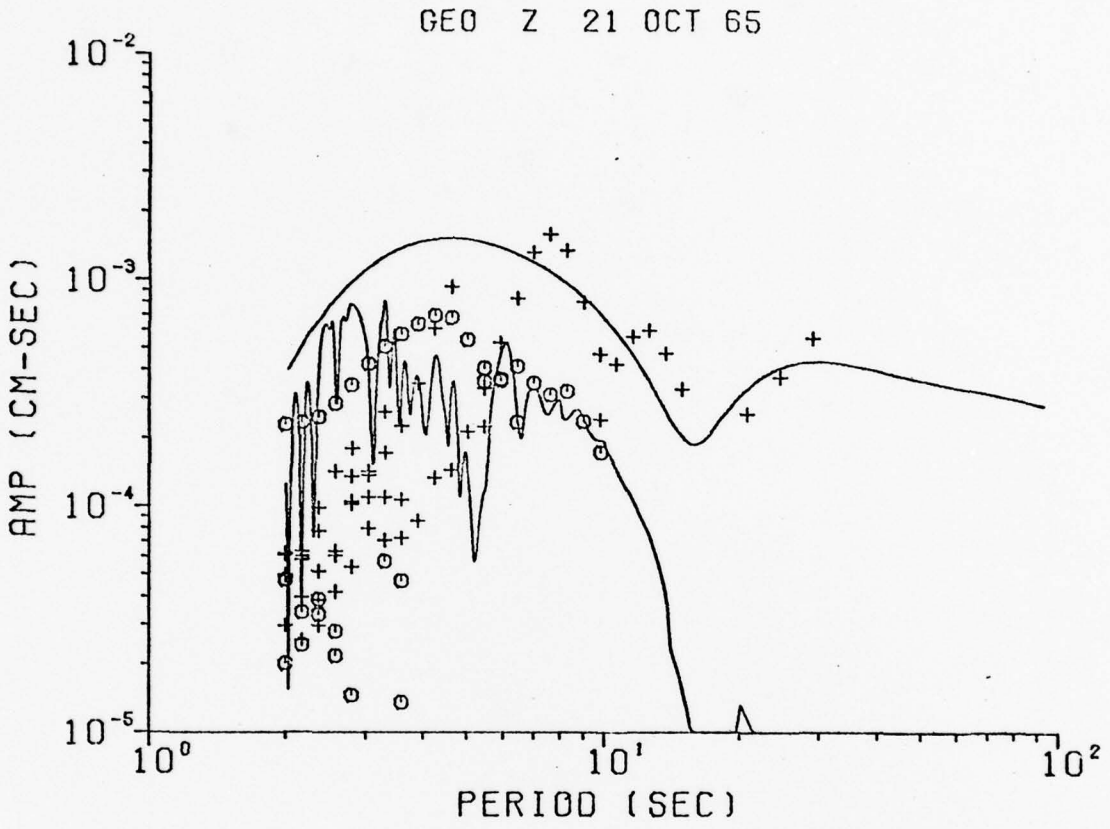

Figure 2. Comparison of theoretical and observational amplitude spectra for an eastern United States path.

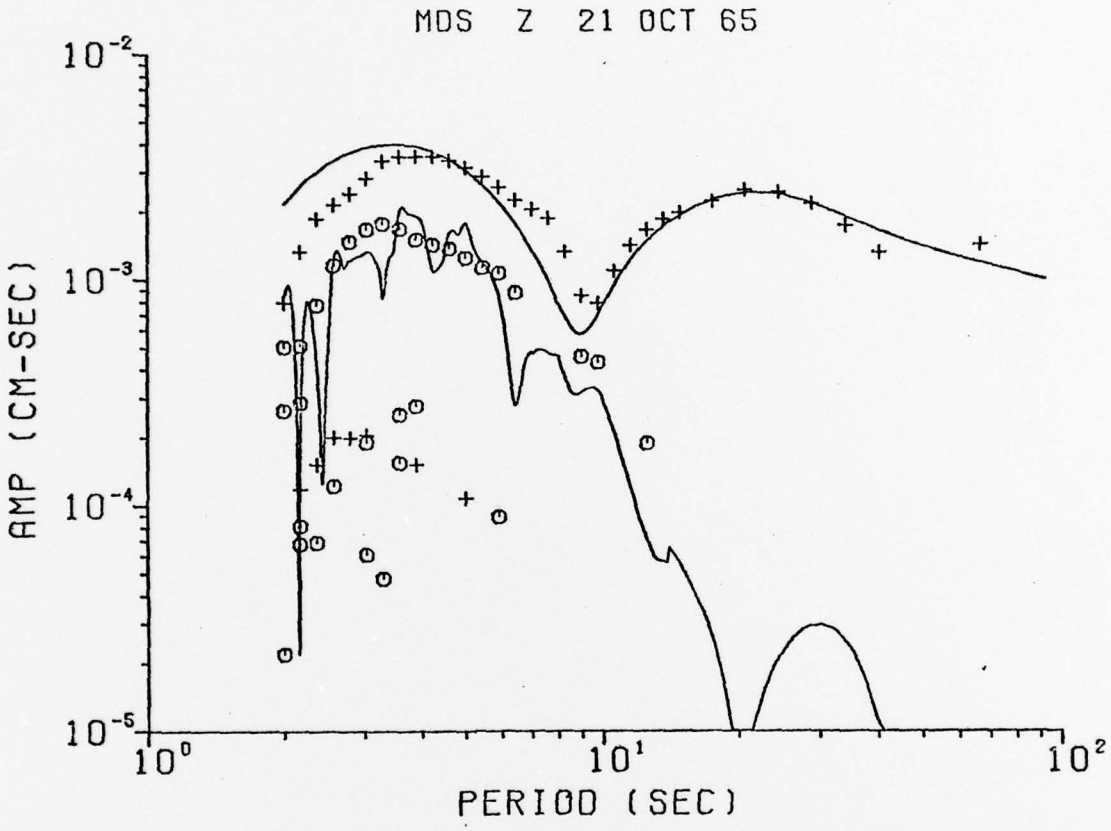

Figure 3. Comparison of theoretical and observational amplitude spectra for an eastern United States path.

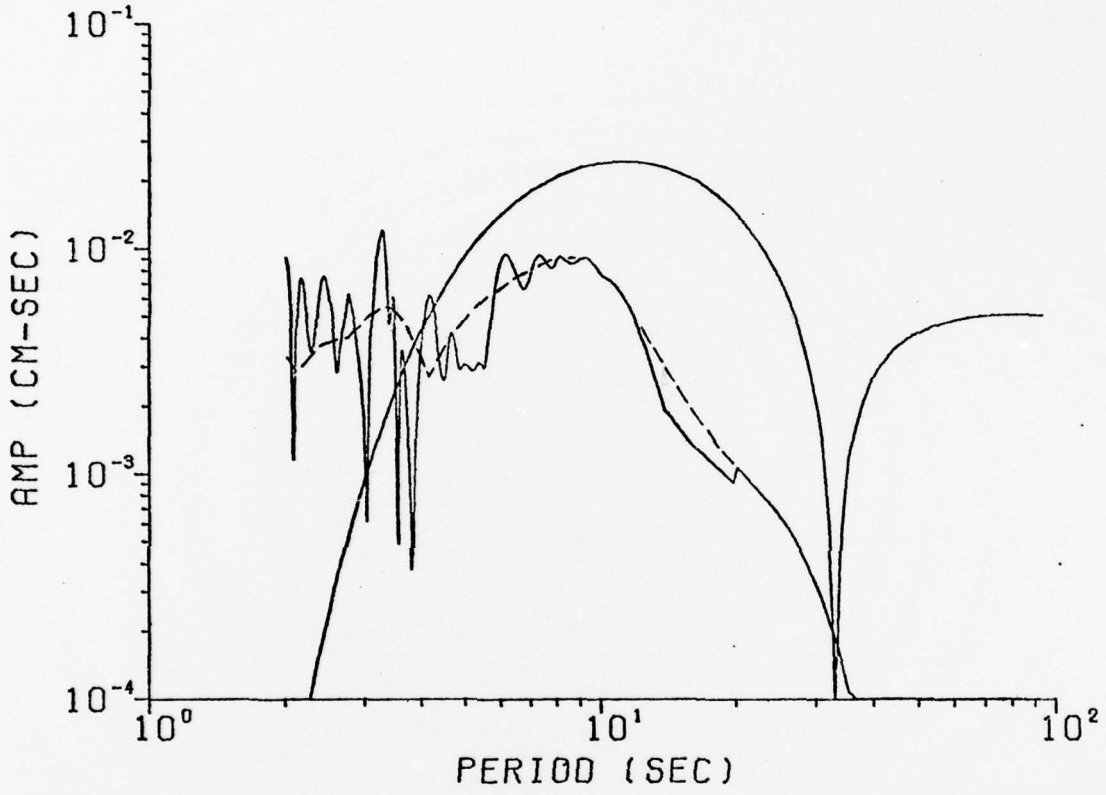

Figure 4. Comparison of the spectrum computed for the net result of the superposition of higher modes and the curve showing the largest value of the amplitudes computed for individual higher modes.

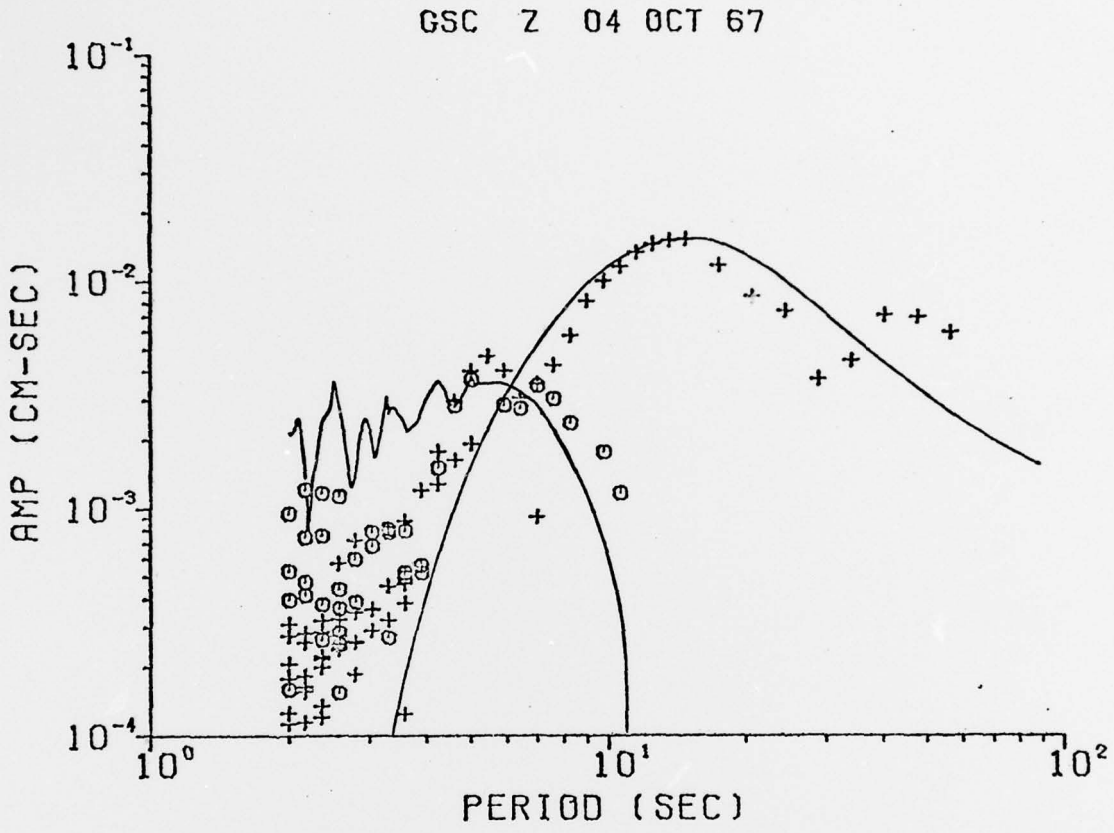

Figure 5. Comparison of theoretical and observational amplitude spectra for a western United States path, using "initial" model in the computation.

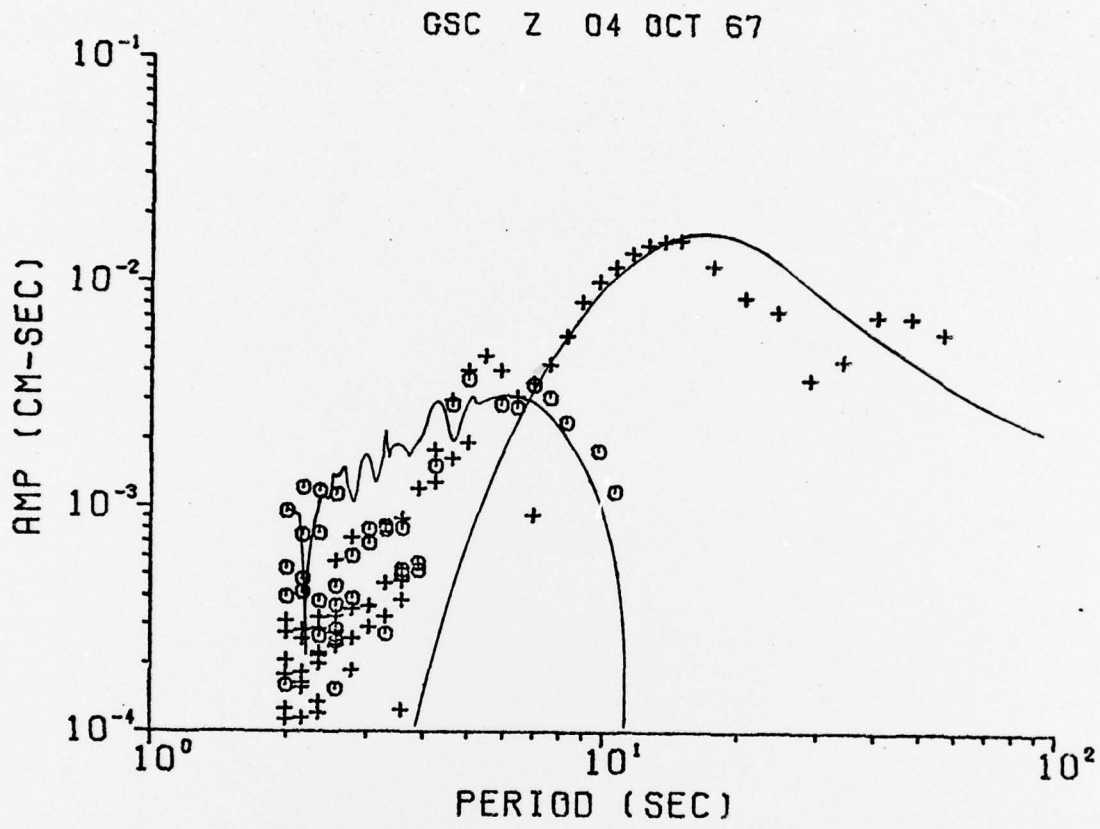

Figure 6. Comparison of theoretical and observational amplitude spectra for the same data as in Figure 5, but using the model obtained after inversion.

Surface Waves and Synthetic Seismograms in the eastern United States

by B.J. Mitchell

The previous semi-annual report presented results of seismic surface wave studies employing both group and phase velocities of Rayleigh and Love waves in the eastern United States. Using modern inversion theory, it was found to be possible to obtain models which adequately explained all of the data and which were isotropic in their elastic properties. The present report will extend those previous results in two ways: (1) by investigating the possibility of higher-mode interference affecting our results, and (2) by investigating the possible existence of fine features in our models through the computation of synthetic seismograms.

Shear velocity models obtained for the eastern United States appear in Figure 1. Although it is possible that polarization anisotropy occurs in the lower crust or upper mantle, as inferred by McEvilly (1965), our results indicate that it is also possible to obtain an isotropic model which explains all of the data. Features of the model include: (1) at least three crustal layers, as previously inferred by Mitchell and Hashim (1977), and (2) an upper mantle which does not require a low-velocity zone. Details of the models obtained from the simultaneous inversion of Rayleigh and Love sources, from Rayleigh waves only, and from Love waves only, are somewhat different. These differences, however, are not significant when the standard deviations and limited resolution of the models are considered.

It could be possible that the Love wave data of our study have been adversely affected by contamination with higher modes (Thatcher and Brune, 1969). The bias produced by this interference could seriously affect our models. We have

investigated this possibility by computing theoretical amplitude spectra corresponding to our eastern United States model for the fundamental- and nine higher modes over the period range 3-50 seconds (Figure 2). It is apparent that over the period range for which we have obtained phase velocity data, there will be no serious interference of the fundamental mode by higher modes.

Figure 1 suggests the existence of two features, which although not resolvable with fundamental-mode data, should be investigated further. They are (1) the low-velocity region in the lower crust which results from the inversion of Rayleigh wave data and from the inversion of the combined Love-Rayleigh data, and (2) the anisotropy which is suggested for the lower crust from the model differences obtained in the separate inversions of Rayleigh and Love wave data. We have attempted to verify or discount the existence of these features by comparing multi-mode synthetic seismograms calculated for our models with observed seismograms at a few stations.

The observed seismograms appear in Figure 3 for stations MDS, AAM, BLA, and ATL. Synthetic seismograms for Rayleigh and Love waves for our models appear in Figure 4. We can match the general features of our seismograms reasonably well. It is apparent however, that differences between the observed and synthetic seismograms are much larger than the differences between the synthetics for the various models. Therefore, the seismogram calculations of Figure 4 indicate that the question of anisotropy in the lower crust cannot be resolved. Similar calculations were performed for models with lower-crustal low-velocity zones. Again it is not possible to decide for or against the existence of that feature.

References

McEvilly, T.V. (1964). Central U.S. crust-upper mantle structure from Love and Rayleigh wave phase velocity inversion, Bull. Seism. Soc. Am., 54, 1997-2015.

Mitchell, B.J., and B.M. Hashim (1977). Seismic velocity determinations in the New Madrid seismic zone: A new method using local earthquakes, Bull. Seism. Soc. Am., 67, 413-424.

Thatcher, W., and J.N. Brune (1969). Higher mode interference and observed anomalous apparent Love wave phase velocities, J. Geophys. Res., 74, 6603-6611.

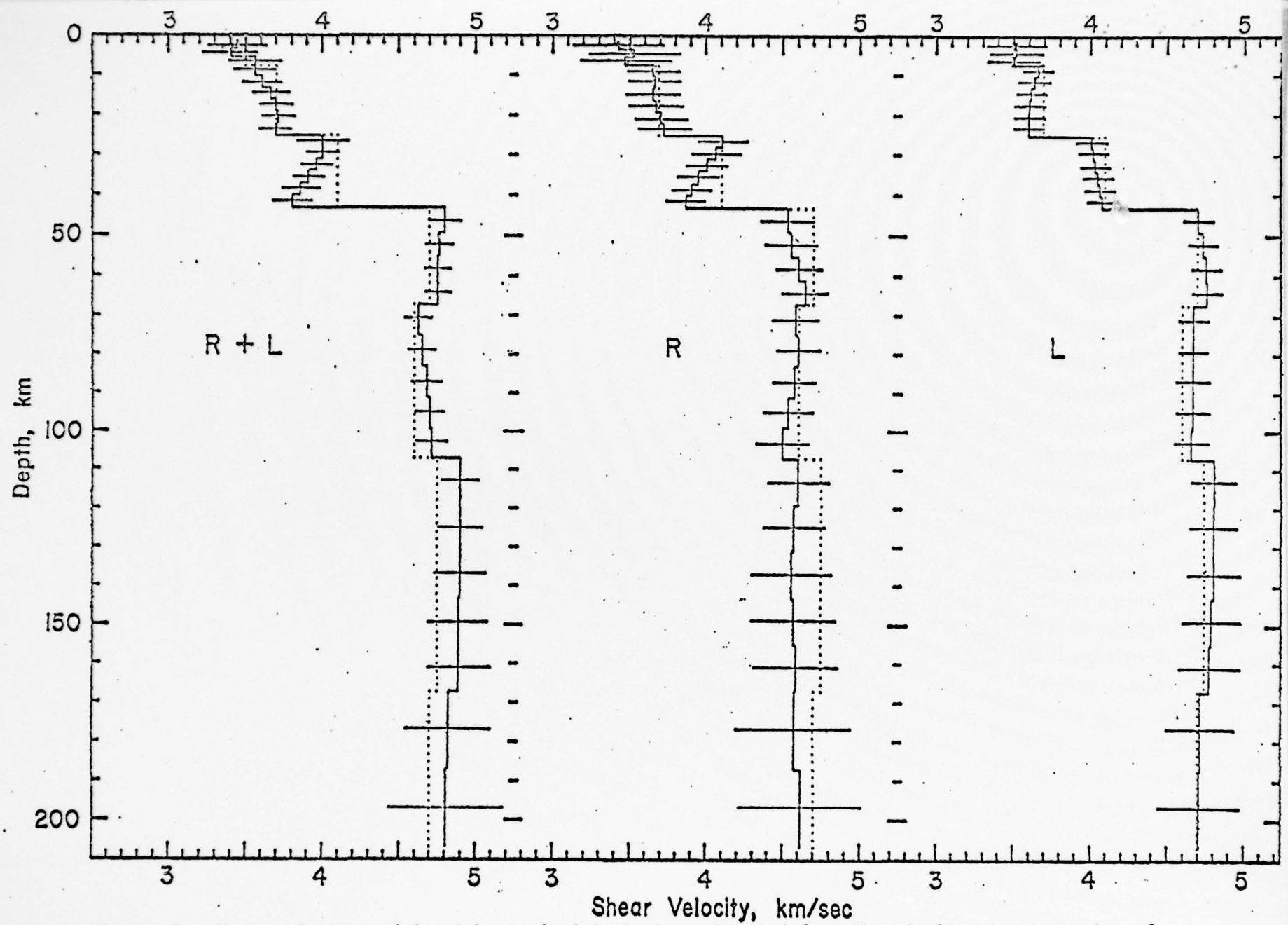

Figure 1. Shear velocity models with standard deviations obtained from the simultaneous inversion of Rayleigh and Love waves (left), from the inversion of Rayleigh waves (center), and from the inversion of Love waves.

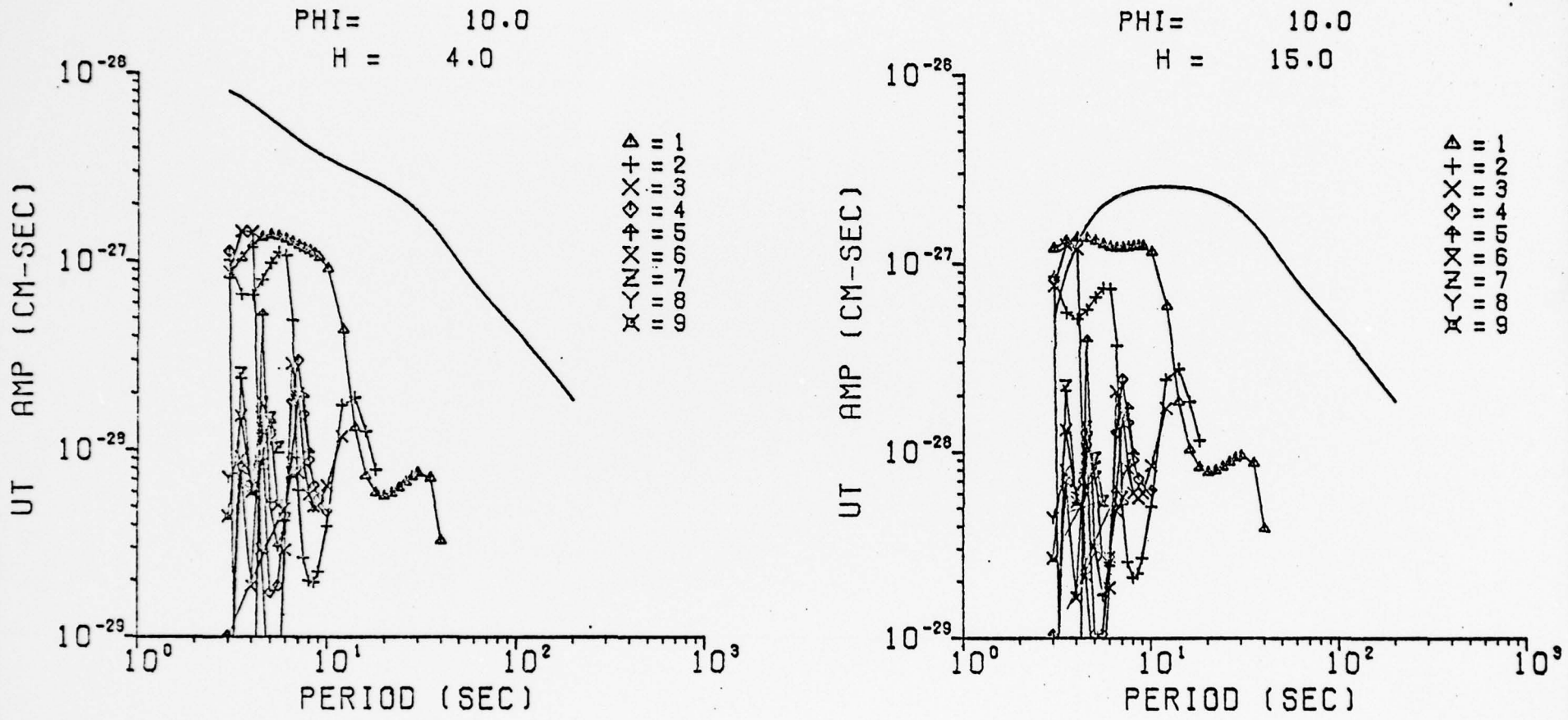

Figure 2. Theoretical amplitude spectra for the fundamental- and nine higher-mode Love waves generated by an earthquake with the fault-plane solution of the event of October 21, 1965. The spectra correspond to focal depths of 4 km (left) and 15 km (right).

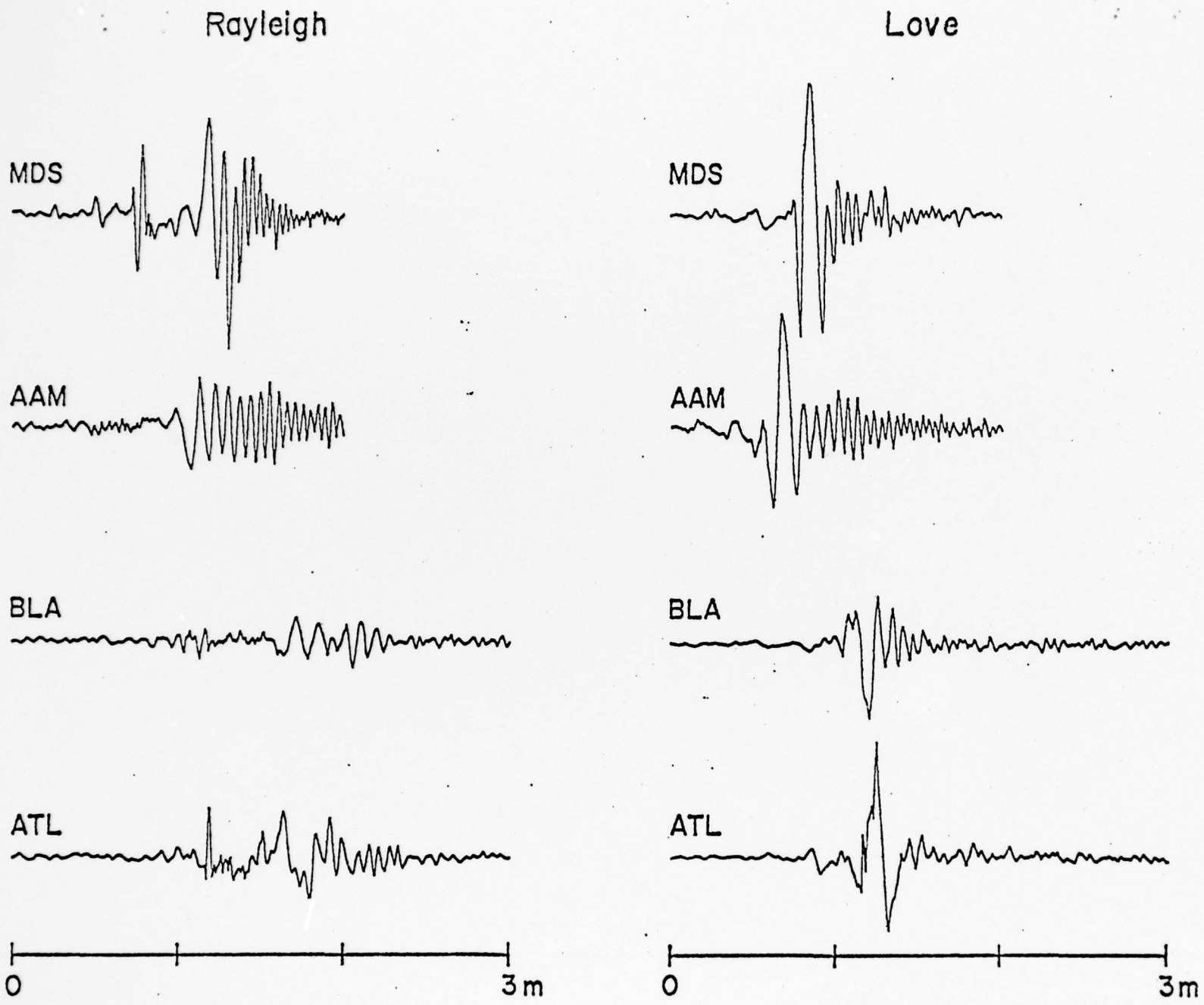

Figure 3. Seismograms observed at stations MDS, AAM, BLA, and ATL for the earthquake of October 21, 1965. Seismograms for transverse motion were obtained from a coordinate transformation of the east-west and north-south components.

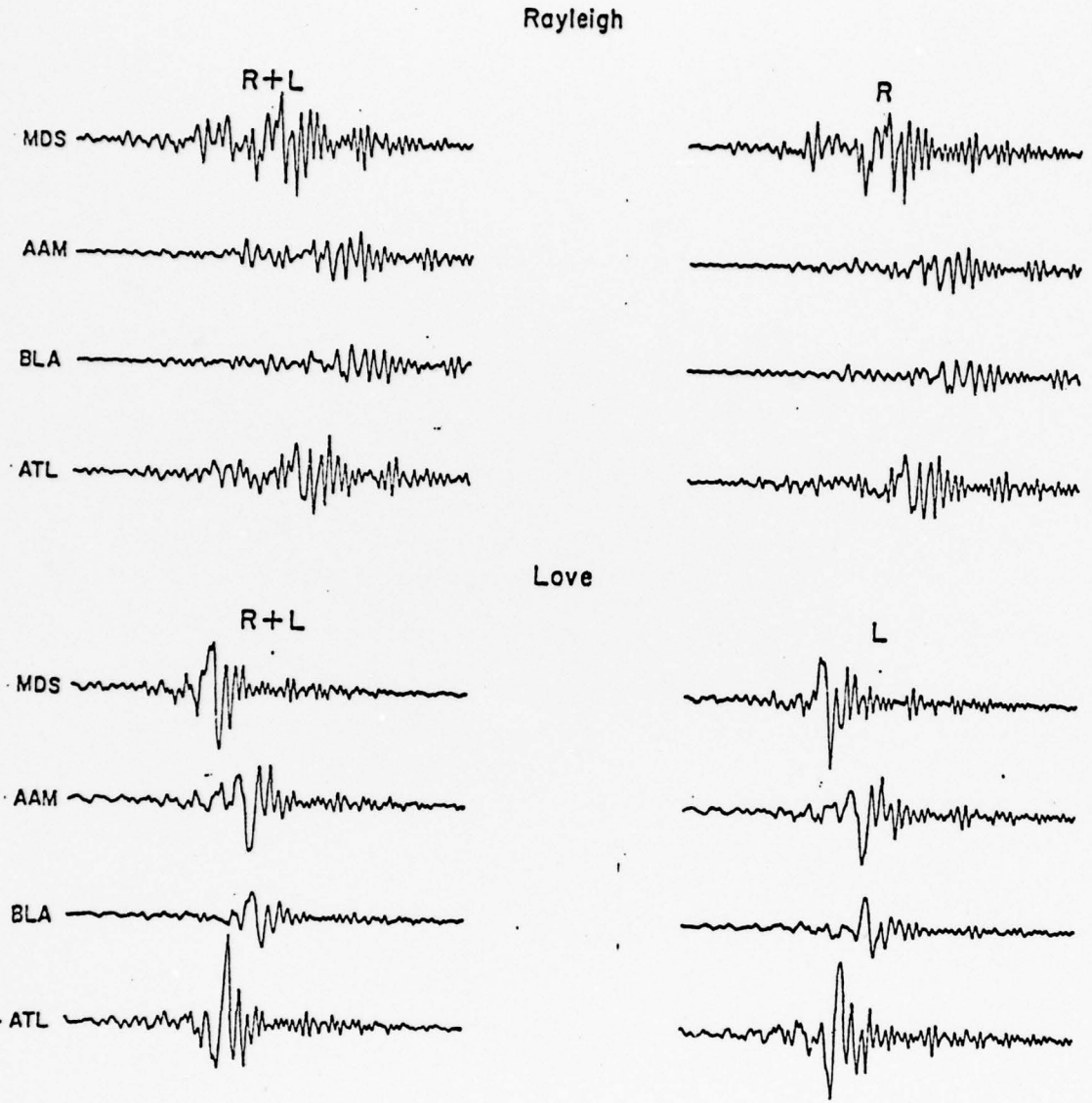

Figure 4. Synthetic seismograms corresponding to the event and stations of Figure 9 for models obtained from a simultaneous inversion of Rayleigh and Love wave data (left), from an inversion of Rayleigh data only (upper right), and from an inversion of Love wave data only. A three minute segment of each seismogram is shown.

Publications for the period 1 March 1973 - 30 September 1978

Street, R.L., R.B. Herrmann, and O.W. Nuttli, Spectral characteristics of the Lg wave generated by central United States earthquakes, Geophys. J. Roy. Ast. Soc., 41, 51-63, 1975.

Herrmann, R.B., and O.W. Nuttli, Ground motion modelling at regional distances for earthquakes in a continental interior, I. Theory and observations, Earth Eng. and Structural Dynamics, 4, 49-58, 1975.

Herrmann, R.B., and O.W. Nuttli, Ground motion modelling at regional distances for earthquakes in a continental interior, II. Effect of focal depth, azimuth and attenuation, Earth Eng. and Structural Dynamics, 4, 59-72, 1975.

Herrmann, R.B., Surface wave generation by central United States earthquakes, Ph.D. Dissertation, Saint Louis Univ., 1974.

Mitchell, B.J., Regional Rayleigh wave attenuation in North America, J. Geophys. Res., 80, 4904-4916, 1975.

Herrmann, R.B., and B.J. Mitchell, Statistical analysis and interpretation of surface wave anelastic attenuation data for the stable interior of North America, Bull. Seism. Soc. Am., 65, 1115-1128, 1975.

Yacoub, N.K., Attenuation of seismic surface waves and its regional variation in the Eurasian continental crust, Ph.D. Dissertation, Saint Louis University, 1976.

Yacoub, N.K., and B.J. Mitchell, Attenuation of Rayleigh wave amplitudes across Eurasia, Bull. Seism. Soc. Am., 67, 751-769, 1977.

Stauder, W., and L. Mualchin, Fault motion in the larger earthquakes of the Kurile-Kamchatka arc and of the Kurile-Hokkaido corner, J. Geophys. Res., 81, 297-308, 1976.

Mitchell, B.J., N.K. Yacoub, and A.M. Correig, A summary of seismic surface wave attenuation and its regional variation across continents and oceans, Am. Geophys. Union Mono 20, The Earth's Crust, 405-425, 1977.

Wen, H.Y., Love waves as an explosion-earthquake discriminant, M.S. Thesis, Saint Louis Univ., 1977.

Yamamoto, J., Rupture processes of some complex earthquakes in southern Mexico, Ph.D. Dissertation, Saint Louis University, 1978.

Nuttli, O.W., Excitation and attenuation of short-period crustal phases in Iran, in preparation, 1978.

Yamamoto, J., and B.J. Mitchell, Source processes of some complex earthquakes in southern Mexico, in preparation, 1978.

Professional Personnel Associated with Research Effort

Faculty

W. Stauder, Professor of Geophysics
O.W. Nuttli, Professor of Geophysics
S. Duda, Professor of Geophysics (now at Univ. of Hamburg)
B.J. Mitchell, Associate Professor of Geophysics

Students

R.B. Herrmann (now on faculty at Saint Louis University)
R.L. Street
L. Mualchin
R. Somayajulu
Y. Yacoub
C.C. Cheng
H.Y. Wen Wang
Y. Yamamoto

Interactions

Papers presented at meetings

Mitchell, B.J., Variation of Rayleigh wave attenuation in eastern and western North America, EOS, Trans. Am. Geophys. Union, 56, 1144, presented at the Fall Annual Meeting, Dec. 12-17, 1974, San Francisco, CA.

Mitchell, B.J., and N.K. Yacoub, Rayleigh wave attenuation in Eurasia, presented at the 71st annual meeting, Cordilleran section, Geol. Soc. Am., March 25-27, 1975, Los Angeles, CA.

Yacoub, N.K., and B.J. Mitchell, Rayleigh wave attenuation and its regional variation within the continental crust of Eurasia, presented at the 47th annual meeting, Eastern section, Seism. Soc. Am., Nov. 6-7, 1975, St. Louis, Mo.

Mitchell, B.J., N.K. Yacoub, and A.M. Correig, Surface wave attenuation and its regional variation across continents and oceans, presented at a symposium on the Nature and Physical Properties of the Earth's Crust, sponsored by the Office of Naval Research and the Colorado School of Mines, Aug. 2-5, 1976, Vail, Colorado.

Mitchell, B.J., Rayleigh wave amplitudes as a tool for determining the thickness and Q values of low-velocity sediments, presented at the 46th Annual Meeting, Soc. Expl. Geophysicists, Oct. 24-28, 1976, Houston, Texas.

Nuttli, O.W., Attenuation of high-frequency Lg waves in the central United States, AFOSR-sponsored meeting on regional discrimination, Dallas, Texas, January, 1978.

Yamamoto, J., and B.J. Mitchell, Source processes associated with some complex earthquakes near the southeastern coast of Mexico, EOS, Trans. Am. Geophys. Union, 59, 326, presented at the annual spring meetig, April 17-21, 1978, Miami, Fla.

Cheng, C.C., and B.J. Mitchell, Q structure of the Colorado Plateau and the Basin and Range province from higher-mode surface wave observations, presented at the Midwest mtg. of the Am. Geophys. Union, Sept. 25-27, 1978, St. Louis, Mo.

Consultative and advisory functions

Air Force Technical Applications Center
Advisory Panel - O.W. Nuttli

Air Force Office of Scientific Research
Proposal Review Panel - O.W. Nuttli

Systems, Science, and Software
Consultant on attenuation of seismic surface waves,
December, 1976 - B.J. Mitchell

(8) (19) REPORT DOCUMENTATION PAGE

READ INSTRUCTIONS BEFORE COMPLETING FORM

1. REPORT NUMBER	2. GOVT ACCESSION NO.	3. RECIPIENT'S CATALOG NUMBER
AFOSR-TR- 79-0456		

4. TITLE (and Subtitle) (6)
Research in Seismology

5. TYPE OF REPORT & PERIOD COVERED (9)
Final rept
1 Mar 73 - 30 Sept 78

6. PERFORMING ORG. REPORT NUMBER

7. AUTHOR(s) (10)
Brian J. Mitchell
Otto W. Nuttli

8. CONTRACT OR GRANT NUMBER(s) (15)
F44620-73-C-0042
ARPA Order-3291

9. PERFORMING ORGANIZATION NAME AND ADDRESS
Dept. of Earth & Atm. Sci.
Saint Louis University
St. Louis, MO 63156

10. PROGRAM ELEMENT, PROJECT, TASK AREA & WORK UNIT NUMBERS
62701E 8F10
(16) AO 3291-11 (17) 11

11. CONTROLLING OFFICE NAME AND ADDRESS (11)
Advanced Research Project Agency/NMR
1400 Wilson Blvd.
Arlington, Virginia 22209

12. REPORT DATE
September, 1978

13. NUMBER OF PAGES
62

14. MONITORING AGENCY NAME & ADDRESS(if different from Controlling Office) (12) 66p.
Air Force Office of Scientific Research/NP
Bolling Air Force Base
Washington, D.C. 20332

15. SECURITY CLASS. (of this report)
Unclassified

15a. DECLASSIFICATION/DOWNGRADING SCHEDULE

16. DISTRIBUTION STATEMENT (of this Report)

Approved for public release. Distribution unlimited.

17. DISTRIBUTION STATEMENT (of the abstract entered in Block 20, if different from Report)

18. SUPPLEMENTARY NOTES

19. KEY WORDS (Continue on reverse side if necessary and identify by block number)
Attenuation
Magnitude
Spectra
Surface waves
Q

20. ABSTRACT (Continue on reverse side if necessary and identify by block number)

Seismic surface wave attenuation was found to vary significantly in different geographical regions of the earth, tectonic regions exhibiting greater attenuation than stable regions. Much of this variation is due to lateral variations of Q structure in the upper crust. For Iran, the attenuation of crustal seismic phases is similar to that of the western United States.

DD FORM 1 JAN 73 1473 EDITION OF 1 NOV 65 IS OBSOLETE

UNCLASSIFIED
SECURITY CLASSIFICATION OF THIS PAGE (When Data Entered)

405 292